MEMO 2-17-59E

NASA MEMO 2-17-59E

NASA

MEMORANDUM

EFFECTS OF EXTERNAL STREAM ON THE PERFORMANCE OF ISENTROPIC PLUG-TYPE NOZZLES AT MACH NUMBERS OF 2.0, 1.8, AND 1.5

By Alfred S. Valerino, Robert F. Zappa, and Kaleel L. Abdalla

Lewis Research Center
Cleveland, Ohio

Declassified March 15, 1962

NATIONAL AERONAUTICS AND SPACE ADMINISTRATION
WASHINGTON
March 1959

NATIONAL AERONAUTICS AND SPACE ADMINISTRATION

MEMORANDUM 2-17-59E

EFFECTS OF EXTERNAL STREAM ON THE PERFORMANCE OF ISENTROPIC PLUG-TYPE NOZZLES AT MACH NUMBERS OF 2.0, 1.8, AND 1.5

By Alfred S. Valerino, Robert F. Zappa, and Kaleel L. Abdalla

SUMMARY

An investigation of the external stream effects on the performance characteristics of several isentropic-plug exhaust nozzles was conducted in the NASA Lewis 8- by 6-foot supersonic tunnel at zero angle of attack through a jet-pressure-ratio range from jet-off to approximately 25 at free-stream Mach numbers of 2.0, 1.8, and 1.5. The variables investigated included nozzle design pressure ratio, ratio of nozzle-throat to maximum body area, and afterbody shape. In addition, the effects of partial internal expansion and of ring-shaped afterbody extensions were studied for a nozzle designed to operate at a pressure ratio of 25.

For nozzles operating at pressure ratios lower than design, low base pressures resulting from the interaction of the jet with a supersonic stream have large adverse effects on thrust.

Over-all performance is improved by increasing the base size to permit more reasonable boattail angles. Improved over-all performance may also be obtained by the incorporation of some internal expansion or by the addition of ring-shaped afterbody extensions to improve the external flow.

As a result of the adverse jet-stream-interaction effects, thrusts predicted from quiescent-air nozzle data become increasingly optimistic as the design pressure ratio increases. Magnitudes of stream effects on thrust for a Mach 3 design nozzle are 9 percent at Mach 1.5 and 3 percent at Mach 2.0.

INTRODUCTION

Exhaust-nozzle types that can provide good thrust characteristics over a wide range of operating pressure ratios are needed for high-speed aircraft and for rocket-powered missile applications. One nozzle type

that has received some attention is the plug-type nozzle in which all or a large part of the expansion occurs externally. Early tests in quiescent air have shown good over-all performance (refs. 1 to 3). However, since the expansion occurs externally, the thrust characteristics are dependent on the external stream, and references 4 and 5 show that adverse affects may be encountered at transonic speeds.

The purpose of this investigation was to determine, at supersonic speeds, the external stream effects on the performance of isentropic-plug exhaust nozzles. The primary parameters investigated were nozzle design pressure ratio, ratio of nozzle-throat to maximum body area, and afterbody shape. In addition, the effects of employing some internal expansion and of adding several types of ringed-shaped fairings, similar to those described in reference 5, were studied.

The investigation was conducted at Mach numbers of 1.5, 1.8, and 2.0 at zero angle of attack. Nozzle jet-pressure ratio was varied from jet-off to a value of approximately 25.

SYMBOLS

A cross-sectional area

C_D drag coefficient, $C_D = D/qA$

C_F thrust coefficient, $C_F = F_{measured}/F_i$

C_p pressure coefficient

D drag

d diameter

F gross thrust

F_i ideal thrust

M Mach number

m mass flow

P total pressure

p static pressure

q dynamic pressure

$(r/R_e)^2$	local plug area parameter
V	velocity, ft/sec
β	boattail angle
θ	internal shroud angle at throat
Φ	exit momentum, $\Phi \equiv mV_e + p_eA_e$

Subscripts:

AB	afterbody (boattail plus base)
BT	boattail
b	base
e	exit
j	jet
max	maximum
n	nozzle
t	throat
0	free stream

NOZZLE-AFTERBODY DESIGN CRITERIA

Nozzle Flow

For maximum thrust at design conditions, the plug-type nozzle is usually designed to produce a uniform, parallel exit stream. The nozzle throat is inclined (fig. 1(a)) and the jet flow expands and turns through an angle equal to the shroud exit angle θ. The exit Mach number M_j, the area ratio A_e/A_t, and the design pressure ratio P_j/p_0 are related through the isentropic relations and θ is the corresponding Prandtl-Meyer angle.

At pressure ratios lower than design and in quiescent air, since there is no fixed outer wall tending to produce overexpansion, the flow can adjust to lower turning angles at the throat (fig. 1(b)). The plug pressures fall to approximately p_0 at point A and then, because of the

curvature of the plug, rise somewhat above p_0 over the downstream portions. As a result (e.g., ref. 1) performance is almost as good at low pressure ratios as it is at design pressure ratio.

Stream Effects

The presence of an external stream can alter plug pressure distributions considerably at low operating pressure ratios. The external stream expands over the afterbody (fig. 1(c)) and reacts with the jet flow producing base pressure p_b that may be considerably below the ambient pressure p_0. As a result, plug pressures continue to fall past point A and reach a low close to p_b at point B. Low base region pressures, therefore, effectively overexpand the jet and thrust is affected adversely.

Afterbody Shape

Because of the dependence of thrust on base pressure, a general study should include the effects of afterbody shape. With plug-type nozzles, however, afterbody selection is largely determined by the design of the inner-flow passage; that is, the design of the nozzle, itself. It has already been noted that the shroud exit angle and the shape of the plug near the throat depend only on design pressure ratio. In addition, in order to avoid local regions of supersonic flow on the plug surface immediately upstream of the throat, a combination of minimum plug turning radius and minimum rate exists at which flow area can be decreased. As a result, the shape of the inner shroud wall in the aft region (fig. 1(d)), as well as the amount by which the nozzle area exceeds the exit area, depends only on nozzle design. In reference 6, for example, it is stated that, in general, nozzle area exceeds exit area by approximately 10 percent.

In general, then, in the aft region, external geometries must lie between those having relatively large boattail angles and those having relatively large bases. The boattail angle in the approach region depends on the nozzle area relative to the maximum body cross-sectional area and is independent of nozzle design.

Configurations Tested

The configurations tested were based on the considerations of the previous section. In order to achieve the best possible external-flow conditions without sacrificing internal performance, plug-turning radius

and internal-flow area were sized to produce a plug-surface Mach number of approximately 0.7 in the region between the throat and maximum plug diameter.

Important Parameters

The important parameters and the range of each were as follows (see also fig. 2 and tables I and II):

Nozzle design pressure ratio. - The nozzles were designed by the method of characteristics for pressure ratios of 10, 15, and 25. These values are of course, in the range of current interest for turbojet applications; moreover, it was felt that the trends with design pressure could also apply to the rocket-missile case. (In the configuration designations of fig. 2 and tables I and II, design pressure ratio is indicated by the first number.)

Throat to maximum body area ratio. - This parameter (the second number of the configuration designation) determines the size of the nozzle relative to the body. A value of 0.2 was chosen as the basic number. Also included for each nozzle was a maximum value of throat to body area ratio that could be obtained without alteration to the body shape upstream of the aft portion. These values were 0.30, 0.25, and 0.20 for nozzles with pressure ratios of 10, 15, and 25, respectively.

Boattail geometry. - Two boattail shapes were included. One had a relatively small base area; the other had a base of sufficient size to permit a 15° aft boattail angle. These are indicated by the letters S and L, respectively, in the configuration designations.

Reduced nozzle throat area. - Several configurations were designed with a closed-down aft shroud, which reduced the nozzle throat area to simulate afterburner-off operation. Thus, the configurations of figures 2(e), (f), and (l) are the afterburner-off versions (identified by the letters AO) of the configurations of figures 2(c), (d), and (k), respectively.

Internal expansion. - The large adverse effects on nozzle performance at pressure ratios lower than design result from the low pressures caused by interaction of the stream with the afterbody and/or jet. This is particularly true for plug-type nozzles in which all of the expansion is taken externally because of the large amounts by which nozzle area exceeds exit area and because of the large boattail angles (as discussed previously in regard to fig. 1(d)).

One possibility for improving the situation is to provide some internal expansion. A nozzle having combined internal and external

expansion can have lower boattail angles, and in many cases the internal overexpansion losses associated with operation at low pressure ratios can be avoided. For example, consider a high Mach number turbojet in which the nozzle pressure ratio at subsonic cruise is about 5 while the desired design pressure ratio is 25. A nozzle having internal expansion through a pressure ratio of 5, with the remainder of the expansion external, should suffer less from stream effects than an all-external-expansion nozzle, because of the improvement in afterbody shape; but, the losses associated with overexpansion of the internal flow should be small and should occur only in the transient condition between takeoff and cruise.

A similar discussion applies to nozzles for rocket-powered missiles. The nozzle can be designed with an internal expansion corresponding to the pressure ratio at which the motor is started, followed by external expansion to the desired design condition.

In order to investigate the improvements that could result from combined external-internal expansion, configuration 25EI-.2-S, (fig. 2(n)) was designed. The letters EI designate partial internal expansion. The nozzle and afterbody parameters are similar to those of configuration 25-.2-S (fig. 2(k)) except in that the amount of internal expansion equivalent to a pressure ratio of 5 was included, which permitted a reduction in boattail angle from $44^{\circ}34'$ to $28^{\circ}39'$.

A somewhat different approach is represented by configuration 25X-.2-S (fig. 2(m)), which is the result of simply adding an internally cylindrical extension of sufficient length to configuration 25-.2-S to permit a boattail angle equal to that of configuration 25EI-.2-S. However, since the extension tends to force the internal flow to expand through the entire design turning angle, overexpansion losses for configuration 25X-.2-S at low pressure ratios can be greater than those of configuration 25EI-.2-S.

Afterbody extensions. - The investigations of reference 5 show that ring-type afterbody extensions improved the off-design nozzle performance at transonic speeds, and so, similar devices were included in the present study. Since the improvement in performance presumably varies with the amount of low-energy body boundary layer that enters the base region, a flush 8-inch ring (fig. 2(o)), an 8.5-inch ring (fig. 2(p)), and an 8.2-inch contoured ring (fig. 2(q)) were included. The contoured ring was arbitrarily designed to have the same boattail angle as those of figures 2(m) and (n).

APPARATUS AND PROCEDURE

A schematic diagram of the jet-exit-model tunnel installation is shown in figure 3. The exit model (fig. 4) consisted of a forebody having a 10° half-angle cone and a cylindrical section with an 8-inch outside diameter, followed by the afterbody section. Total model length was 71.0 inches, excluding the plug projection.

Air for the model internal flow was predried to a dewpoint of -40° F. This air was obtained from an external source and supplied to the model through the two hollow support struts.

Force Measurements

The axial-force-measuring system consisted of a strain-gage link in parallel with a pressurized bellows. This system permitted the use of a smaller strain-gage link and provided increasing accuracy. The floating and grounded portions of the model are indicated in figure 4.

Pressurized air to the bellows was regulated to nullify the strain-gage-link force. The effective area of the bellows was precalibrated experimentally.

Instrumentation

The location of instrumentation for a typical afterbody configuration is shown in figure 5. The model base forces were obtained from four static-pressure orifices located circumferentially in the base 90° apart. The boattail drag was determined by integration of the two rows of seven static-orifices. The static-pressure distribution on the exit plug was obtained from thirteen static-pressure orifices on the plug surface.

Data Reduction

The nozzle thrust minus total drag was obtained from the strain-gage reading, from the summation of internal pressure-area terms, and from the bellows calibration. The nozzle thrust was computed by adding the model total drag to the term for model thrust minus total drag. The model total drag was determined by adding the following: the jet-off total drag minus the base drag, the difference between jet-off and jet-on boattail drag, and the jet-on base drag.

The afterbody drag was the sum of measured boattail and base drags. The drag of the 8.2-inch contoured ring was obtained from the integration

of two rows of static-pressure orifices, one row facing the boattail surface of the configuration, the other row located externally opposite the first row. For the two flat rings, the drag was obtained by subtracting the jet-off total drag minus base drag of the identical configurations without the rings from the jet-off total drag minus base drag of the configurations with rings. The effect of the exhaust jet on the drag of the flat rings was assumed negligible.

The values of thrust and thrust minus drag were compared with the ideal thrust where ideal thrust was computed from the measured jet weight flow, total temperature, total pressure, and the free-stream static pressure, assuming complete isentropic expansion. Jet weight flow was obtained by subtracting the calibrated leakage flow from the total weight flow measured from calibrated ASME sharp-edged orifice plates. Jet total temperature was measured by two thermocouples in the model pressure bottle. Jet total pressure was calculated from jet weight flow, jet temperature, and the measured static pressure and area at model station 60.

RESULTS AND DISCUSSION

The external stream effects on nozzle thrust, boattail and base-drag coefficients as well as on the ratio of base to free-stream static pressures for each configuration are presented in figure 6. For comparative purposes, quiescent-air thrust coefficients were superimposed on these curves. The quiescent-air data of configurations designed to operate at jet pressure ratios of 10 and 15 were obtained from reference 1; those for a design pressure ratio of 25 are estimated values.

In the discussion that follows, general trends over the range of jet pressure ratios at each Mach number will be discussed despite the fact that for any particular application a fixed Mach number - pressure ratio schedule would usually exist.

Thrust

Usually, at the lower jet pressure ratios, the thrusts of the various configurations decrease as Mach number increases. This trend, of course, simply reflects the lower base pressures at the higher Mach numbers and results from the fact that thrust, as conventionally defined, is the difference between two independent terms

$$F \equiv \Phi - p_0 A_e$$

where Φ is the exit momentum. In dimensionless quantities,

$$\frac{F}{P_j A_t} \equiv \frac{\Phi}{P_j A_t} - \frac{p_0}{P_j}\frac{A_e}{A_t}$$

The last term in the thrust definition clearly depends only on the jet pressure ratio, P_j/p_0. The first term, on the other hand, should depend essentially on the "effective jet pressure ratio," P_j/p_b. In quiescent-air tests, $p_b = p_0$ and $P_j/p_0 = P_j/p_b$ so that nozzle performance depends only on jet pressure ratio; in a stream, however, p_b does not in general equal p_0 and furthermore, the ratio p_b/p_0 varies with Mach number so that, as was seen in figure 6, thrust changes with Mach number even at constant jet pressure ratio.

Thrust also varies with Mach number at constant effective jet pressure ratio, as can be seen in figure 7 in which dimensionless thrust and exit momentum are presented at several Mach numbers as functions of effective jet pressure ratio for a typical configuration (10-.2-S). As Mach number increases thrust decreases. Momentum, on the other hand, is independent of Mach number when plotted as a function of effective jet pressure ratio. Because of this property, exit momentum ($\Phi = F + p_0 A_e$) is a useful parameter in an investigation of stream effects and in the checking of results during the data-reduction process.

Plug Pressures

The plug pressure distributions of figure 8 explain the effects of stream Mach number on thrust more graphically perhaps than the momentum parameter. For configuration 10-.2-S, the ratios of local plug pressures to jet total pressure are plotted as functions of the local plug area parameter $(r/R_e)^2$. Curves are presented (fig. 8) for Mach numbers of 2.0 and 1.5 at jet pressure ratios of 2, 4, and 10. Also shown are the ratios of base pressures (solid symbols) to jet total pressure.

At a pressure ratio of 2 (fig. 8(a)), which is low relative to the design value of 10, as stream Mach number increases from 1.5 to 2.0, base pressure drops from 0.49 P_j to 0.26 P_j. As a result, plug pressures fall from values above 0.6 P_j to as low as 0.37 P_j. The area between the two curves indicates the thrust difference between Mach 1.5 and Mach 2.0 operation and was found to be in excellent agreement with the measured difference indicated in figure 6(a).

At a pressure ratio of 4 (fig. 8(b)) the effect of stream Mach number is similar except that at the higher pressure ratio, base pressures can affect only the downstream portions of the plug. Finally, at a design pressure ratio of 10 (fig. 8(c)), plug pressures are completely unaffected by changes in base pressure.

Effect of Design Pressure Ratio

Thrust coefficient is plotted in figure 9 as a function of pressure ratio at Mach numbers of 1.5, 1.8, and 2.0 for a series of nozzles that have different design pressure ratios but are otherwise similar. At low pressure ratios two effects are apparent: (1) the higher the design pressure the greater the thrust loss due to stream effects and (2) the higher the stream Mach number (and therefore, the lower the base pressure) the greater the thrust loss.

The nature of the relation between thrust and design pressure is obvious if the data are replotted as a function of relative pressure ratio, that is, the ratio of the actual pressure ratio to the design pressure ratio, as shown in figure 10. The broken curve represents the theoretical thrust for a fully overexpanded jet corrected to an on-design thrust coefficient of 0.98. At Mach 2 all configuration data fall on a single curve and are in excellent agreement with the theoretical values. At Mach 2, therefore, base pressures are sufficiently low to produce a completely overexpanded jet; at Mach 1.5 the amount of overexpansion is less severe except for the configuration with a pressure ratio of 25.

Effects of Afterbody Shape

The limits on afterbody shape set by nozzle design have been discussed previously. Typical effects of boattail angle and relative base size are shown in figure 11 in which configurations having large boattail angles but small bases (the S configurations) are compared with those having a more reasonable boattail angle of 15° but somewhat larger bases (the L configurations). Thrust minus drag and the ratio of thrust to ideal thrust, as well as total afterbody drag are plotted as functions of jet pressure ratio. At both Mach 2.0 (fig. 11(a)) and 1.5 (fig. 11(b)) the drag of the L configuration is lower and, since thrusts are about the same, thrust minus drag is higher. This same result also applies to the other configurations, as can be seen by comparing the curves of figures 6(c) and (d), 6(g) and (h), or 6(i) and (j). In all cases, the lower boattail drags of the L configurations more than offset the base-drag differences.

The relative magnitudes of the factors that affect the afterbody drags can be observed from the local pressure distributions along the boattail and on the base, plotted in figure 12. It can be seen that the boattail pressures for the L configuration are relatively independent of jet pressure ratio whereas those for S configuration are greatly influenced by the changes in base pressure that accompany changes in jet pressure ratio.

Since the area under the curves represents drag, the lower total drag of the L configuration clearly results mainly from the lower boattail drags; the differences in base drags of the two configurations are small compared with the differences in boattail drags.

Effect of Ratio of Throat to Maximum Body Area

The ratio of throat to maximum body area determines the projected afterbody area relative to the maximum area and also affects the shape of the approach section of the afterbody (fig. 1(d)). A typical comparison of effects of large and small nozzles (configurations 10-.3-S and 10-.2-S) on performance is given in figure 13.

At Mach 2 (fig. 13(a)) the high drag of configuration 10-.2-S simply reflects the large projected afterbody area and no other effects are apparent. At Mach 1.5 (fig. 13(b)), however, a reversal in drag trends as well as a noticeable effect on thrust occurs at low pressure ratios. Thrust minus drag for configuration 10-.2-S is actually higher over a small range of pressure ratios near 4, despite the larger projected area.

The reversal in trends is, of course, a direct consequence of base-pressure effects as can be seen by comparing the Mach 1.5 data curves of figures 6(a) and (c). Since similar results occur for the other configurations of figure 6, perhaps the most important point is that, although in general larger nozzles have lower drags and thrusts that are less sensitive to stream effects, the trends can reverse in a manner that is difficult to generalize.

Afterburner-Off Operation

The effects of closing down the shroud on configurations 10-.3-S, 10-.3-L, and 25-.2-S in order to reduce throat area for afterburner-off operation can be obtained by comparing figures 6(c) and (e), 6(d) and (f), or 6(k) and (l). The results can be summarized quite simply: for the afterburner-off configurations thrust decreases because of the poor nozzle configuration and drag increases because of the increased base area.

Nozzle and Afterbody Modifications

Nozzle modifications consisting of the addition of internal expansion and afterbody modifications consisting of ring-type extensions were investigated on the nozzle with a design pressure ratio of 25 in an attempt to reduce adverse stream effects at low pressure ratios. The performance of the basic configuration and the modifications is given in figures 6(k) and 6(m) to (q). For comparative purposes, thrust, drag, and thrust minus drag are replotted in figure 14.

For the basic, unmodified configuration (25-.2-S), thrust is good at high pressure ratios but poor at low pressure ratios especially at Mach 1.5 and the drag is high at all conditions. Modification to provide some internal expansion (configuration 25EI-.2-S) results in good thrust and low drags and provides the best performance at all conditions except for pressure ratios below approximately 6 and Mach 1.5.

The configuration for which a lower boattail angle was achieved by a shroud extension (25X-.2-0) exhibited poor performance because thrust losses more than offset drag reductions. The thrust losses were to be expected at low pressure ratios because the shroud extension forced the jet to overexpand. At a pressure ratio of 22 at Mach 2.0, however, there is no obvious explanation for measured thrust coefficients as low as 0.95.

The ring configurations were intended to improve drag at all conditions and thrust at low pressure ratios by allowing low-energy air to bleed into the base region; that is, the rings were to combine "base bleed" and "ejector action". The configurations tested, however, were essentially a "first try" at supersonic speeds and as a result may not be the best obtainable with this technique.

Considering first the flat rings and drag effects, it can be seen that improvements in afterbody drag vary from slight at Mach 2.0 to appreciable at Mach 1.5. In fact, at Mach 1.5 and for pressure ratios below approximately 11 the 8-inch ring had the lowest drag of all the configurations. Thrust improvements varied from zero at Mach 2.0 to 10 percent at Mach 1.5. As a result, thrust-minus-drag improvements varied from zero at Mach 2.0 to 20 percent at Mach 1.5.

For the contoured ring, drags were about the same or slightly higher than for the basic configuration; thrust at low pressure ratios was better. Thrust-minus-drag improvements varied from 8 percent at Mach 2.0 to 15 percent at Mach 1.5. Larger extensions to permit still lower boattail angles, as well as variations in the inlet size, are interesting possibilities for future investigations.

Typical Magnitudes for Stream Effects

In order to estimate the magnitudes of stream effects on thrust and hence the magnitude of the error that would result from the use of quiescent-air nozzle data, a Mach number - pressure ratio schedule was chosen. The assumed pressure ratios were those of a typical turbojet and at Mach numbers of 1.5, 1.8, and 2.0 were 6, 8, and 10, respectively. The results are shown in figure 15.

For all nozzles with a pressure ratio of 10, which are on-design at Mach 2.0, no errors exist for Mach numbers down to 1.5. For the nozzles with a pressure ratio of 15, quiescent-air data would overestimate the thrust by as much as 3 percent at Mach 1.5. Finally, for the nozzles with a pressure ratio of 25 (design Mach number, ≈ 3.0) the error depends on configuration; typical values, however, vary from 3 percent at Mach 2.0 to 9 percent at Mach 1.5.

SUMMARY OF RESULTS

The investigation of the external stream effects on the performance of isentropic-plug exhaust nozzles over a Mach number range from 1.5 to 2.0 and a pressure ratio range from jet-off to approximately 25, indicated the following general trends:

1. Low base pressures resulting from the interaction of the jet with a supersonic stream can have large adverse effects on thrust for nozzles operating at pressure ratios lower than design. At Mach 2.0, for example, as a result of the low base pressures a nozzle designed for pressure ratio of 25 can be completely overexpanded at a pressure ratio as low as 5.

2. Increasing the base size to permit more reasonable boattail angles gave over-all performance improvements.

3. Incorporation of some internal expansion or addition of ring-shaped afterbody extensions to improve the external flow improved over-all performance by amounts up to 8 percent at Mach 2.0 and 20 percent at Mach 1.5.

4. As a result of the adverse jet-stream-interaction effects, thrusts predicted from quiescent-air nozzle data become increasingly optimistic with increasing design pressure ratio above 10. For example, quiescent-air thrusts for a nozzle having a design pressure ratio of 25 are too high by 9 percent at Mach 1.5 and 3 percent at Mach 2.0.

Lewis Research Center
National Aeronautics and Space Administration
Cleveland, Ohio, November 24, 1958

REFERENCES

1. Krull, H. George, and Beale, William T.: Effect of Plug Design on Performance Characteristics of Convergent-Plug Exhaust Nozzles. NACA RM E54H05, 1954.

2. Krull, H. George, and Beale, William T.: Effect of Outer-Shell Design on Performance Characteristics of Convergent-Plug Exhaust Nozzles. NACA RM E54K22, 1955.

3. Krull, H. George, and Beale, William T.: Comparison of Two Methods of Modulating the Throat Area of Convergent Plug Nozzles. NACA RM E54L08, 1955.

4. Salmi, R. J., and Cortright, E. M., Jr.: Effects of External Stream Flow and Afterbody Variations on the Performance of a Plug Nozzle at High Subsonic Speeds. NACA RM E56F11a, 1956.

5. Salmi, Reino J.: Preliminary Investigation of Methods to Increase Base Pressure of Plug Nozzles at Mach 0.9. NACA RM E56J05, 1956.

6. Krull, H. George, Beale, William T., and Schmiedlin, Ralph F.: Effect of Several Design Variables on Internal Performance of Convergent-Plug Exhaust Nozzles. NACA RM E56G20, 1956.

TABLE I. - CONFIGURATION PARAMETERS

Configuration		Design jet pressure ratio, $(P_j/p_0)_{design}$	Ratio of throat area to maximum body area, A_t/A_{max}	Ratio of base area to maximum body area, A_b/A_{max}	Ratio of base diameter to jet diameter, d_b/d_j	Internal shroud angle at throat, θ
Designation	Figure 2					
10-.2-S	(a)	10	0.2	0.12	1.14	30°30'
10-.2-L	(b)	↓	.2	.19	1.23	15°
10-.3-S	(c)		.3	.17	1.14	30°30'
10-.3-L	(d)		.3	.29	1.23	15°
10-.21-SAO	(e)		.21	.29	1.28	30°30'
10-.21-LAO	(f)		.21	.40	1.37	15°
15-.2-S	(g)	15	.2	.14	1.14	37°06'
15-.2-L	(h)	↓	.2	.24	1.23	15°
15-.25-S	(i)		.25	.18	1.14	37°06'
15-.25-L	(j)		.25	.29	1.23	15°
25-.2-S	(k)	25	.2	.11	1.08	44°34'
25X-.2-O	(m)	↓	.2	0	1.00	28°39'
25-.2-S (8.2-in. contoured ring)	(q)		.2	.11	1.08	44°34'
25-.2-S (8-in. flat ring)	(o)		.2	.11	1.08	44°34'
25-.2-S (8.5-in. flat ring)	(p)		.2	.11	1.08	44°34'
25-.14-SAO	(l)		.2	.15	1.12	44°34'
25EI-.2-S	(n)		.2	.07	1.05	28°39'

TABLE II. - PLUG COORDINATES

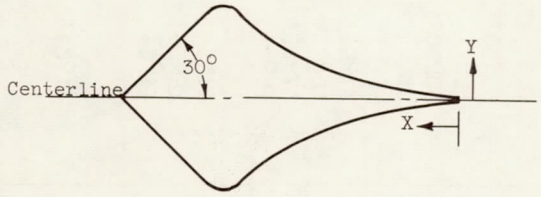

Configuration

10-.2-S
10-.2-L

X	Y
0.000	0.098
.500	.180
1.000	.300
1.500	.450
2.00	.640
2.500	.868
3.000	1.160
3.500	1.521
3.878	1.850

Configuration

10-.3-S
10-.3-L
10-.21-SAO
10-.21-LAO

X	Y
0.000	0.115
.500	.200
1.000	.310
1.500	.445
2.000	.610
2.500	.805
3.000	1.039
3.500	1.318
4.000	1.645
4.500	2.040
4.748	2.265

Configuration

15-.2-S
15-.2-L

X	Y
0.000	0.102
.500	.183
1.000	.283
1.500	.402
2.000	.548
2.500	.720
3.000	.920
3.500	1.158
4.000	1.455
4.250	1.634
4.500	1.832
4.750	2.061
4.907	2.220

Configuration

15-.25-S
15-.25-L

X	Y
0.000	0.111
.500	.195
1.000	.291
1.500	.406
2.000	.542
2.500	.701
3.000	.884
3.500	1.095
4.000	1.344
4.500	1.645
5.000	2.020
5.491	2.481

Configuration

25-.2-S
25X-.2-0
25-.2-S(8.2-in. contoured ring)
25-.2-S(8-in. flat ring)
25-.2-S(8.5-in. flat ring)
25-.14-SAO

X	Y
0.000	.100
.500	.231
1.000	.369
1.500	.500
2.000	.636
2.500	.771
3.000	.907
3.500	1.051
4.000	1.211
4.500	1.398
5.000	1.612
5.500	1.878
6.000	2.222
6.500	2.680
6.687	2.894

Configuration

25EI-.2-S

X	Y
0.000	0.100
.500	.231
1.000	.369
1.500	.500
2.000	.636
2.500	.771
3.000	.907
3.500	1.051
4.000	1.211
4.500	1.398
5.000	1.612
5.500	1.878
5.750	2.035
6.000	2.200
6.250	2.380
6.500	2.560
6.750	2.667
7.000	2.912
7.357	3.172

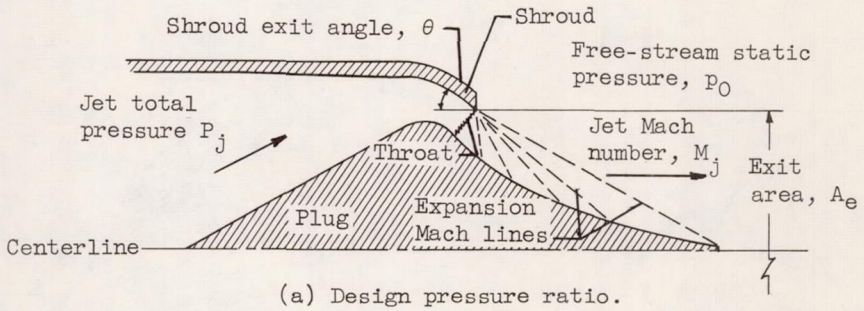

(a) Design pressure ratio.

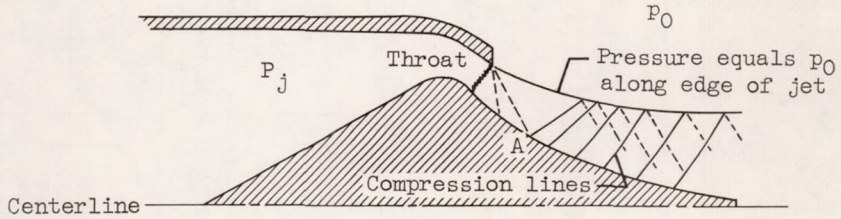

(b) Pressure ratio lower than design pressure. Quiescent air.

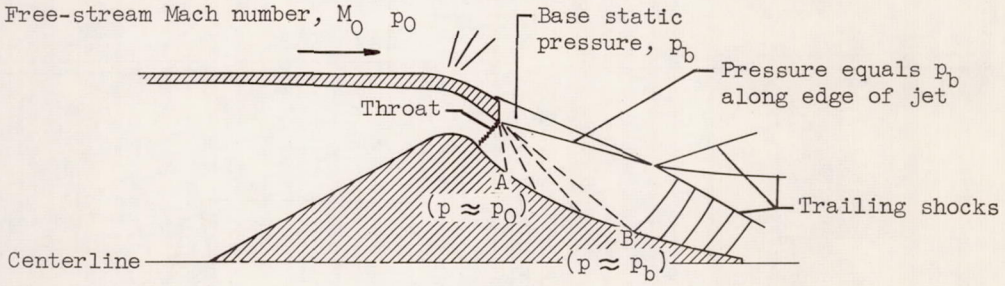

(c) Pressure ratio lower than design. Stream effects.

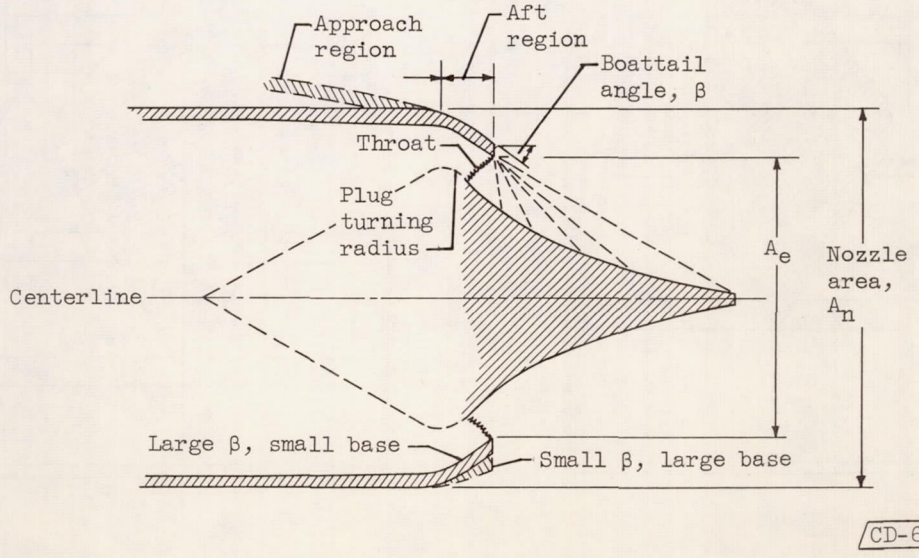

(d) Design details.

Figure 1. - Plug nozzle design considerations.

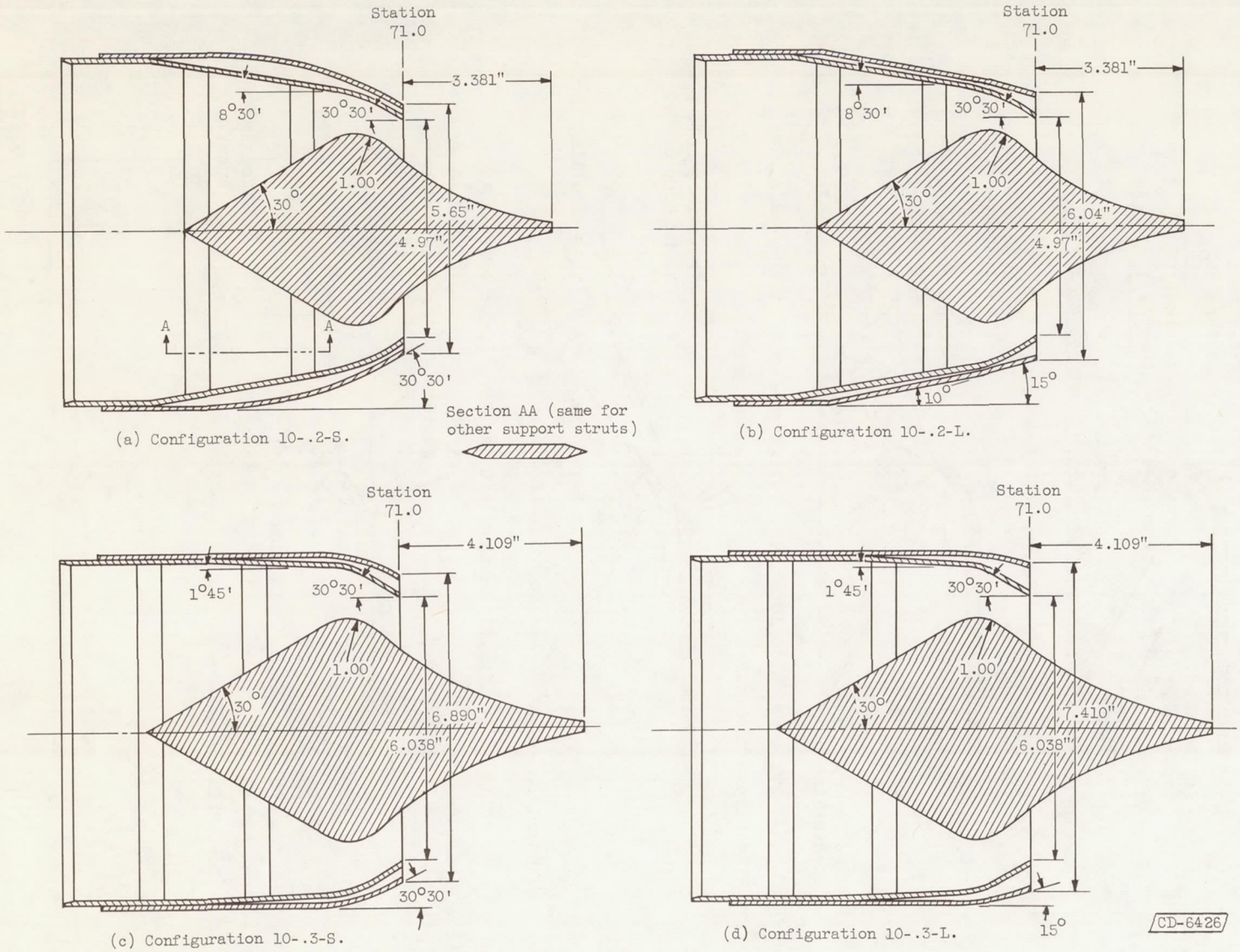

(a) Configuration 10-.2-S.

(b) Configuration 10-.2-L.

(c) Configuration 10-.3-S.

(d) Configuration 10-.3-L.

Figure 2. - Schematic diagrams of nozzle configurations.

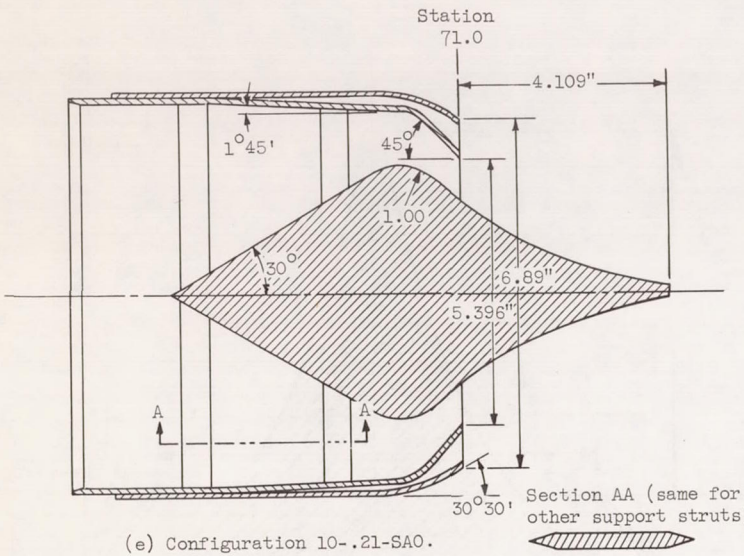

(e) Configuration 10-.21-SA0.

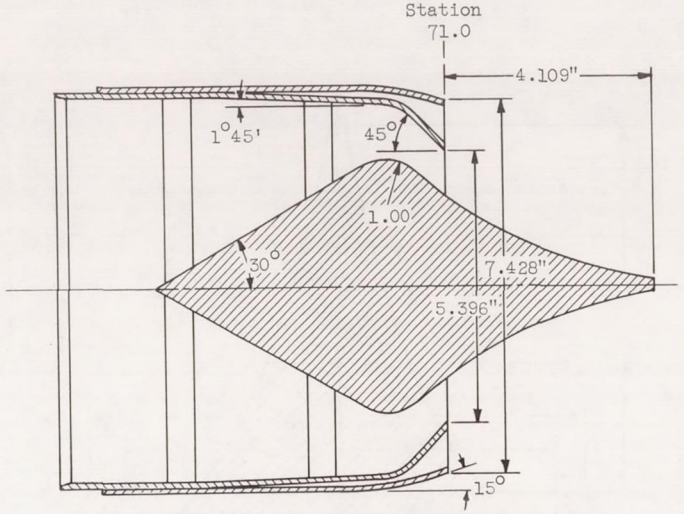

(f) Configuration 10-.21-LA0.

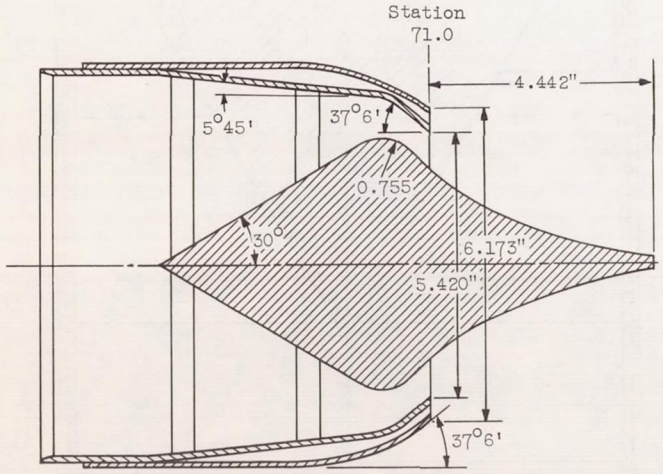

(g) Configuration 15-.2-S.

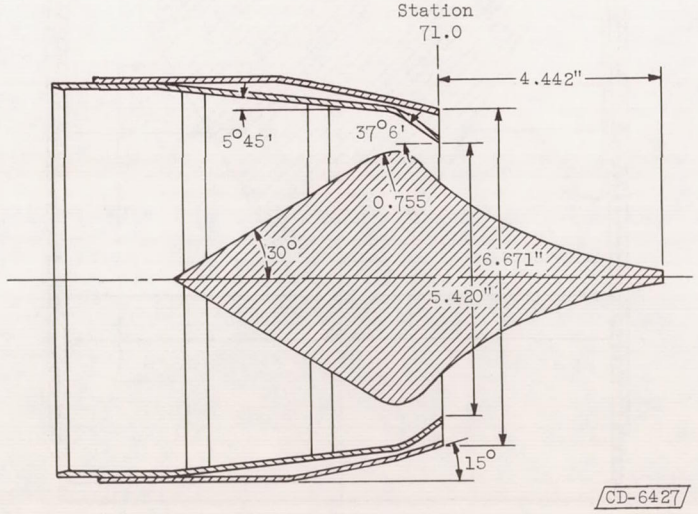

(h) Configuration 15-.2-L.

Figure 2. - Continued. Schematic diagrams of nozzle configurations.

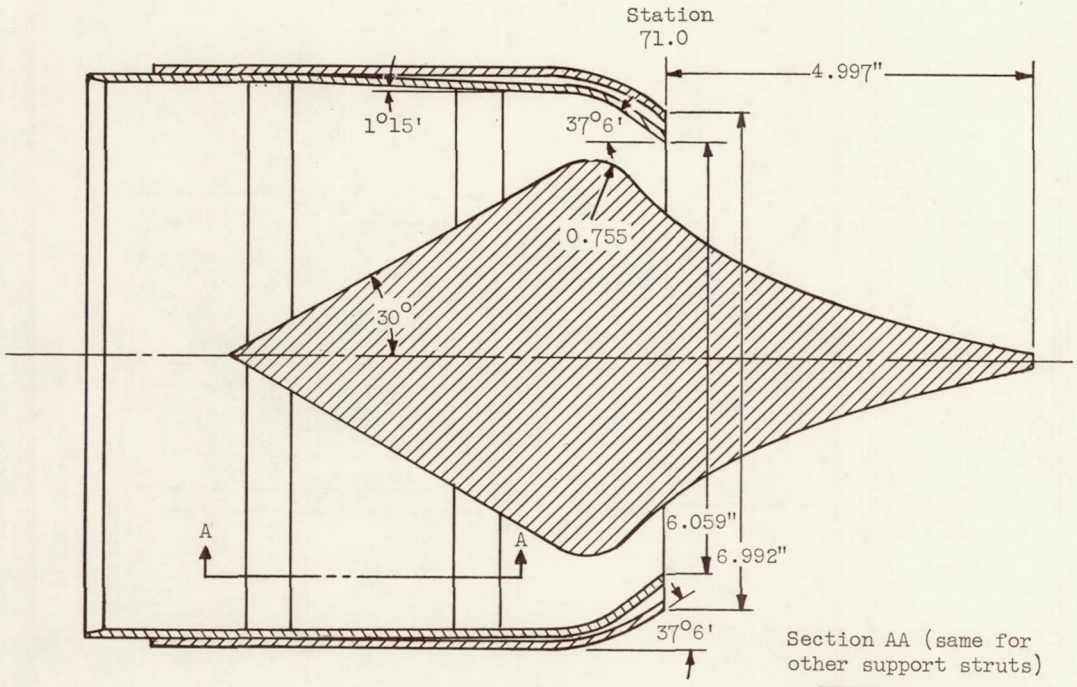

(i) Configuration 15-.25-S.

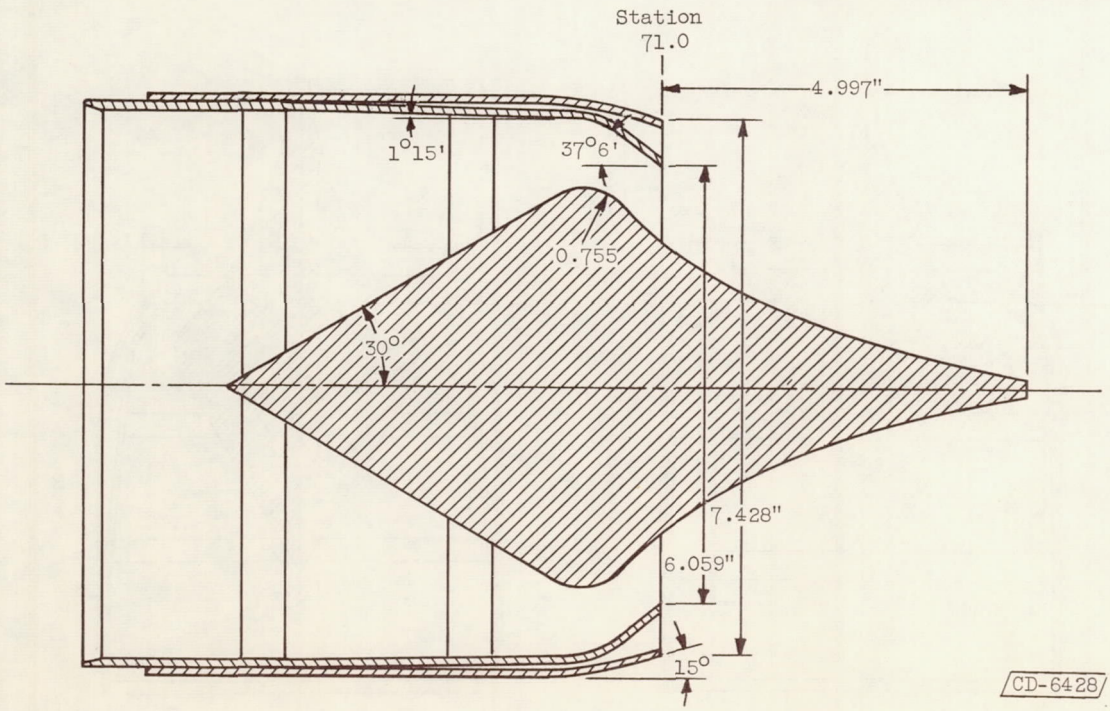

(j) Configuration 15-.25-L.

Figure 2. - Continued. Schematic diagrams of nozzle configurations.

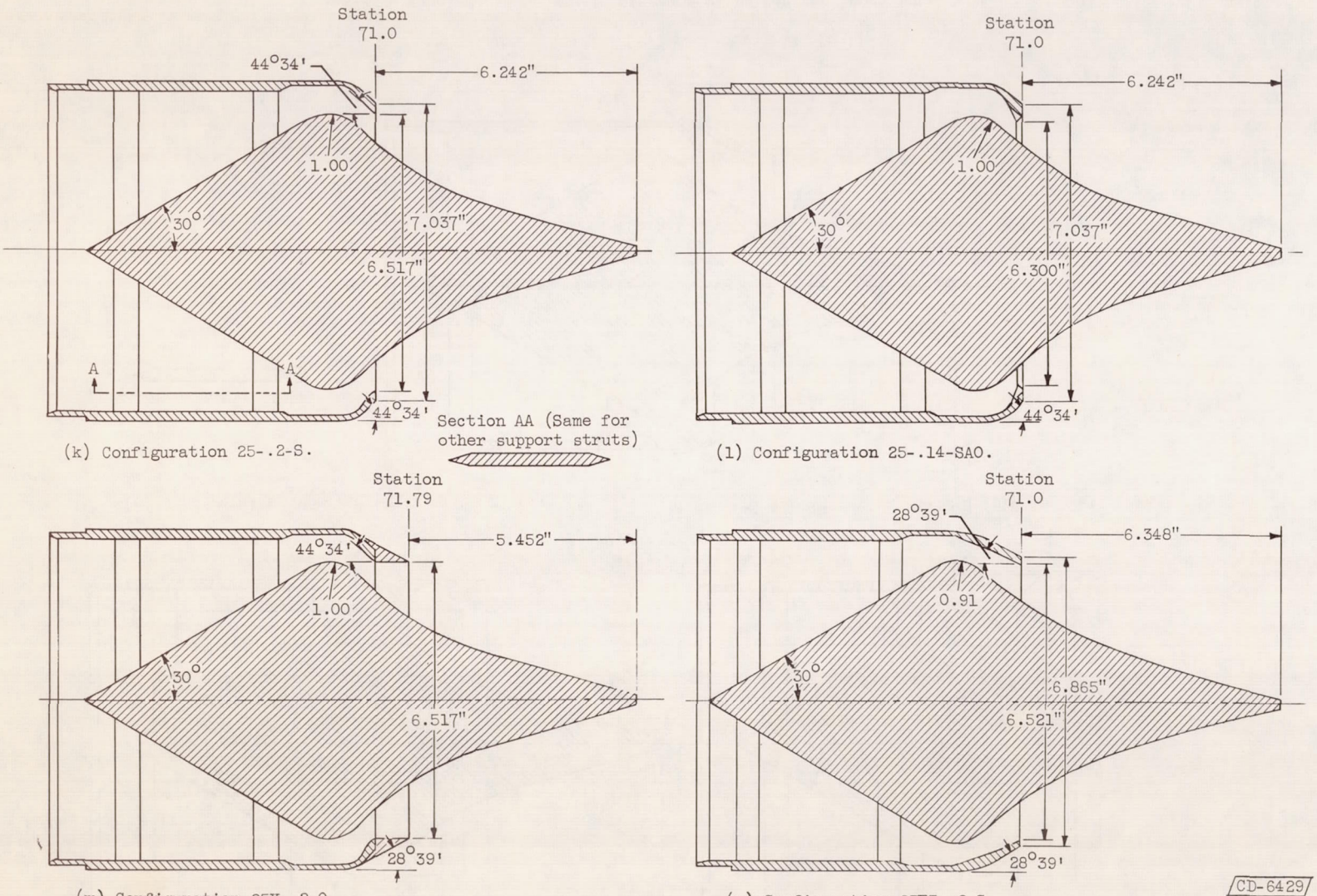

Figure 2. - Continued. Schematic diagrams of nozzle configurations.

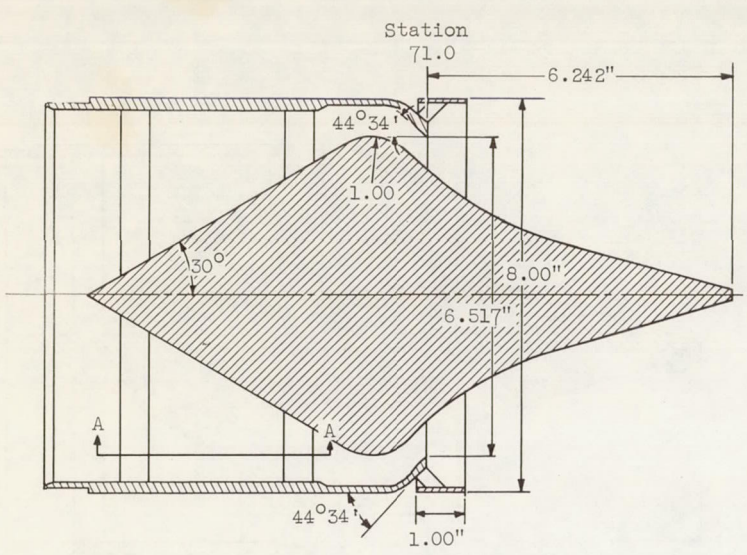

(o) Configuration 25-.2-S (8-in. flat ring).

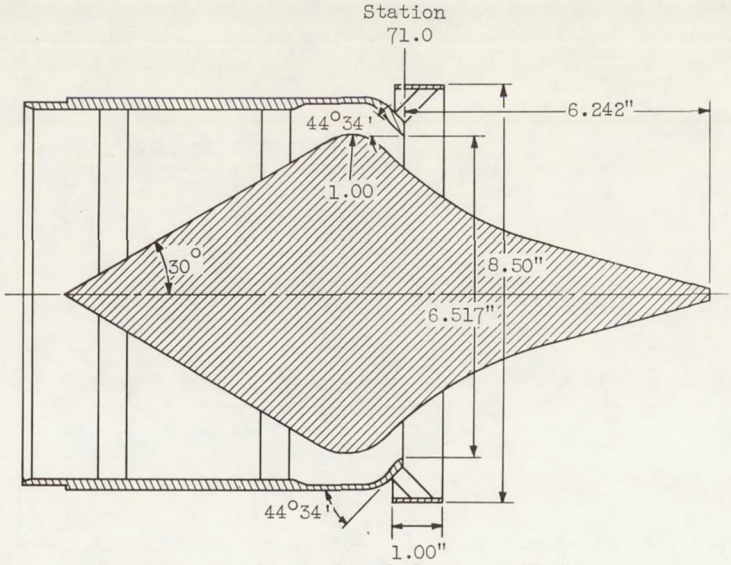

(p) Configuration 25-.2-S (8.5-in. flat ring).

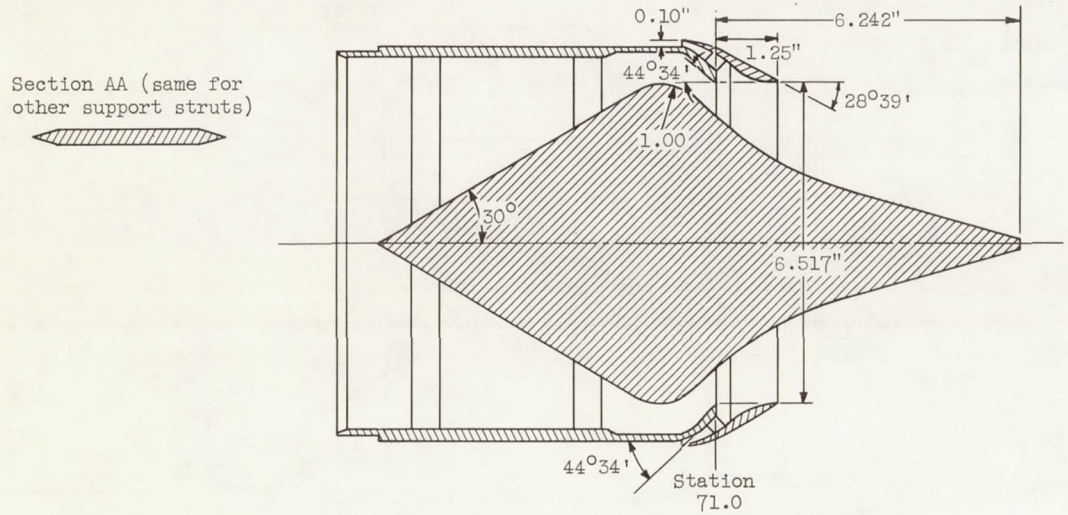

(q) Configuration 25-.2-S (8.2-in. contoured ring).

CD-6430

Figure 2. - Concluded. Schematic diagrams of nozzle configurations.

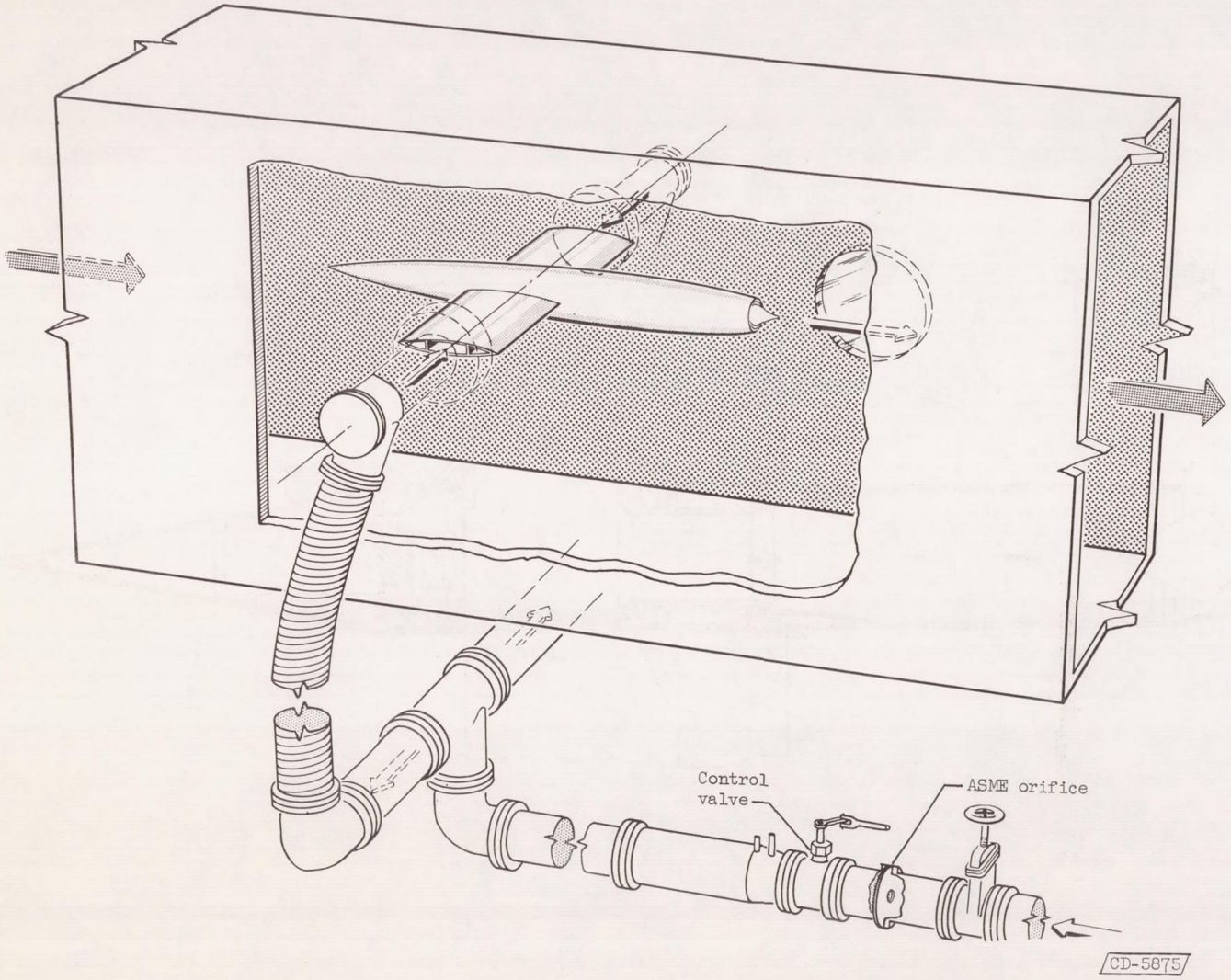

Figure 3. - Schematic diagram of jet-exit-model tunnel installation.

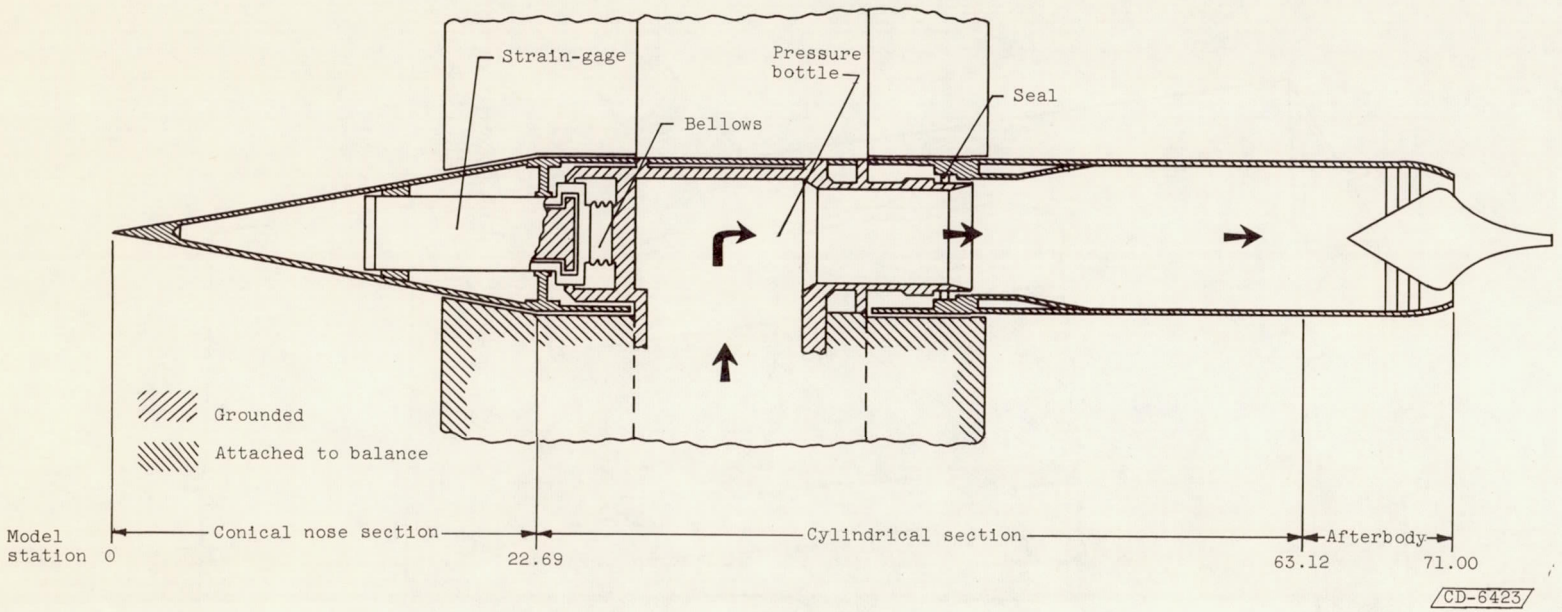

Figure 4. - Schematic diagram of jet exit model.

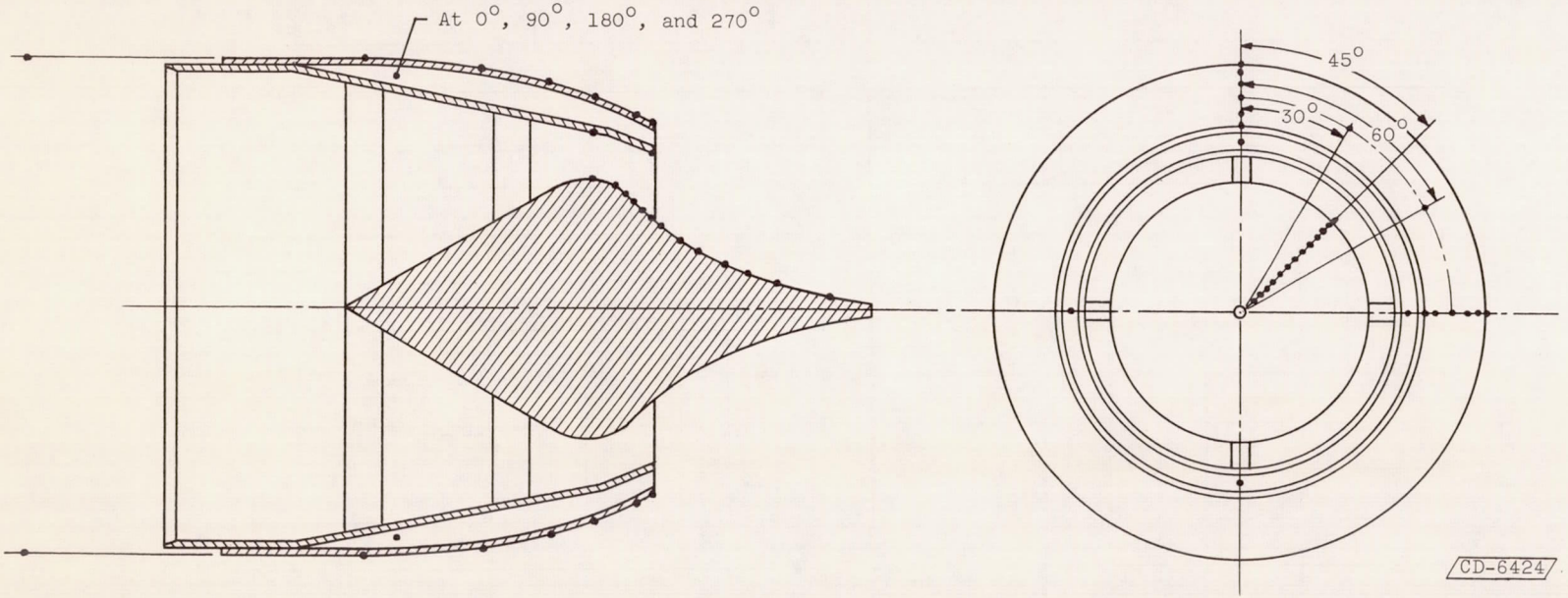

Figure 5. - Location of afterbody instrumentation.

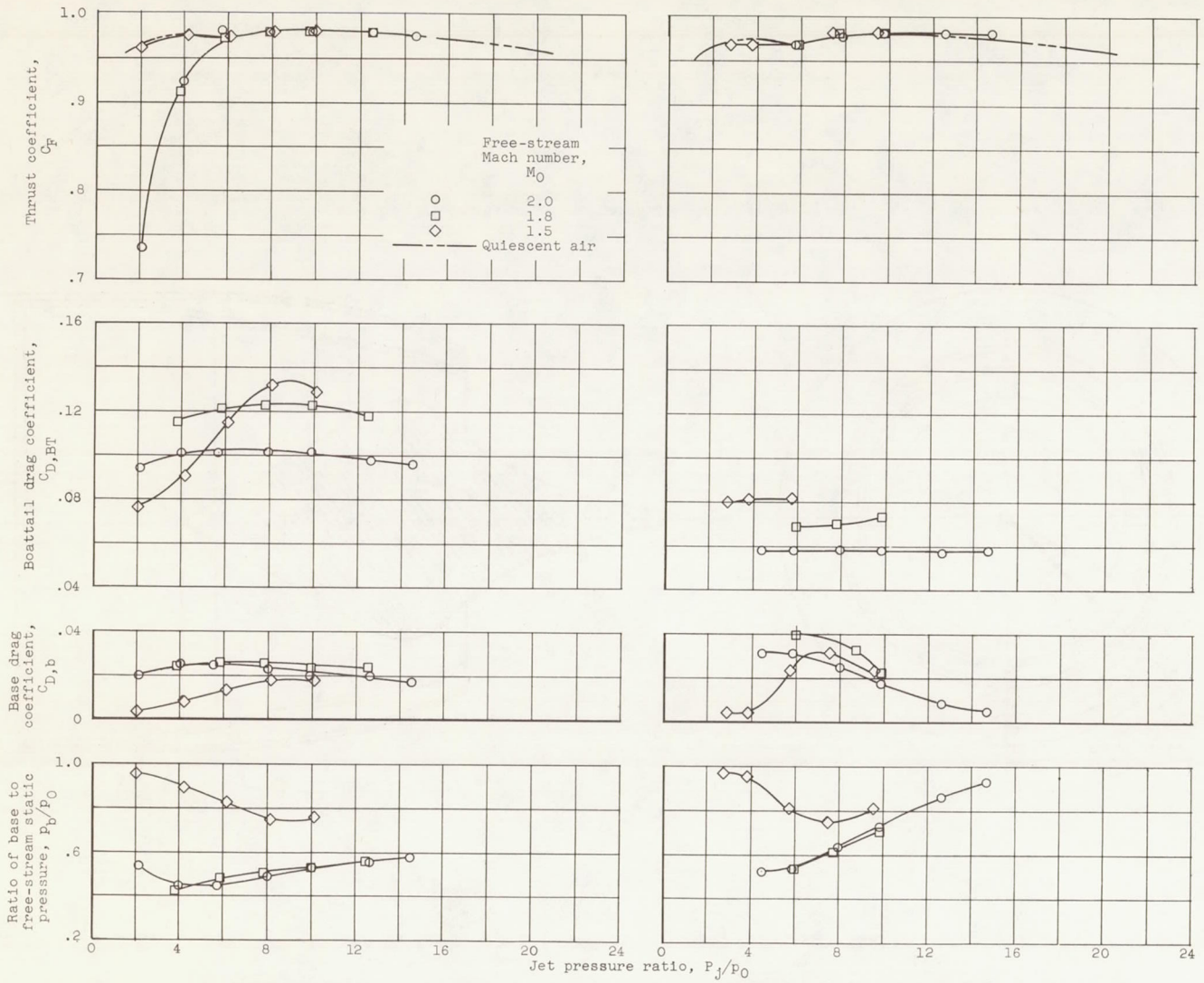

(a) Configuration 10-.2-S.

(b) Configuration 10-.2-L.

Figure 6. - Plug nozzle performance parameters.

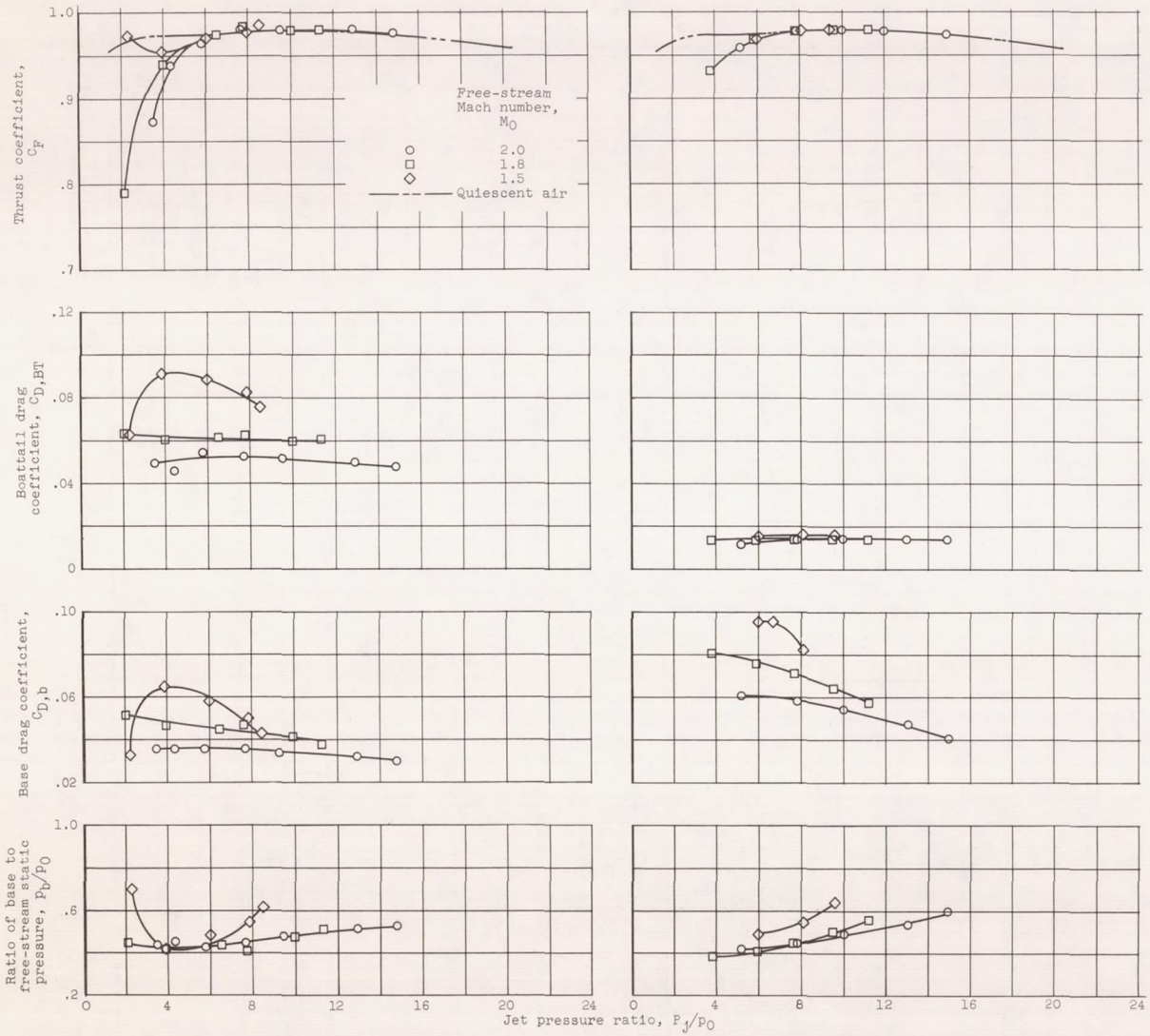

(c) Configuration 10-.3-S.

(d) Configuration 10-.3-L.

Figure 6. - Continued. Plug nozzle performance parameters.

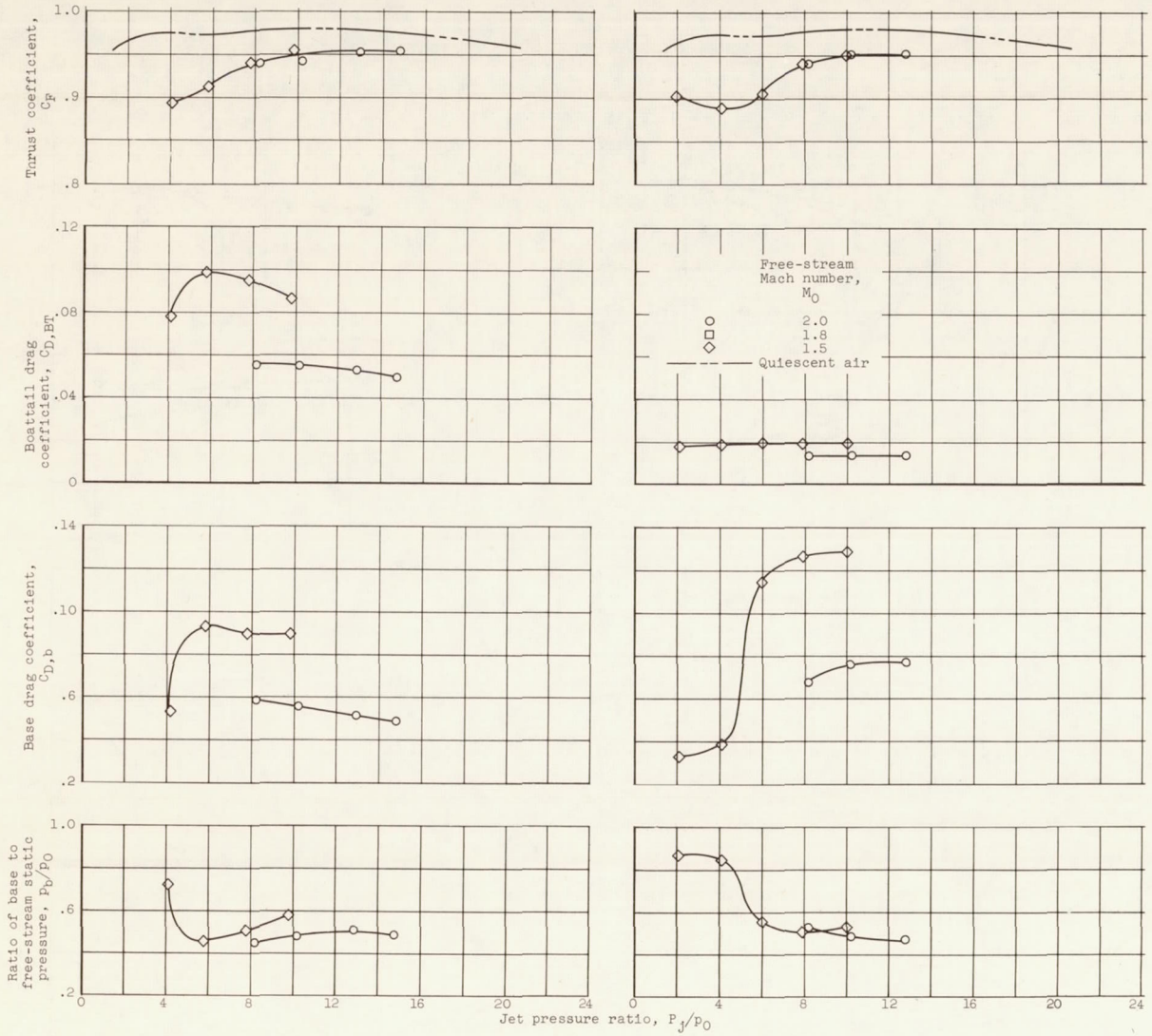

(e) Configuration 10-.21-SA0.

(f) Configuration 10-.21-LA0.

Figure 6. - Continued. Plug nozzle performance parameters.

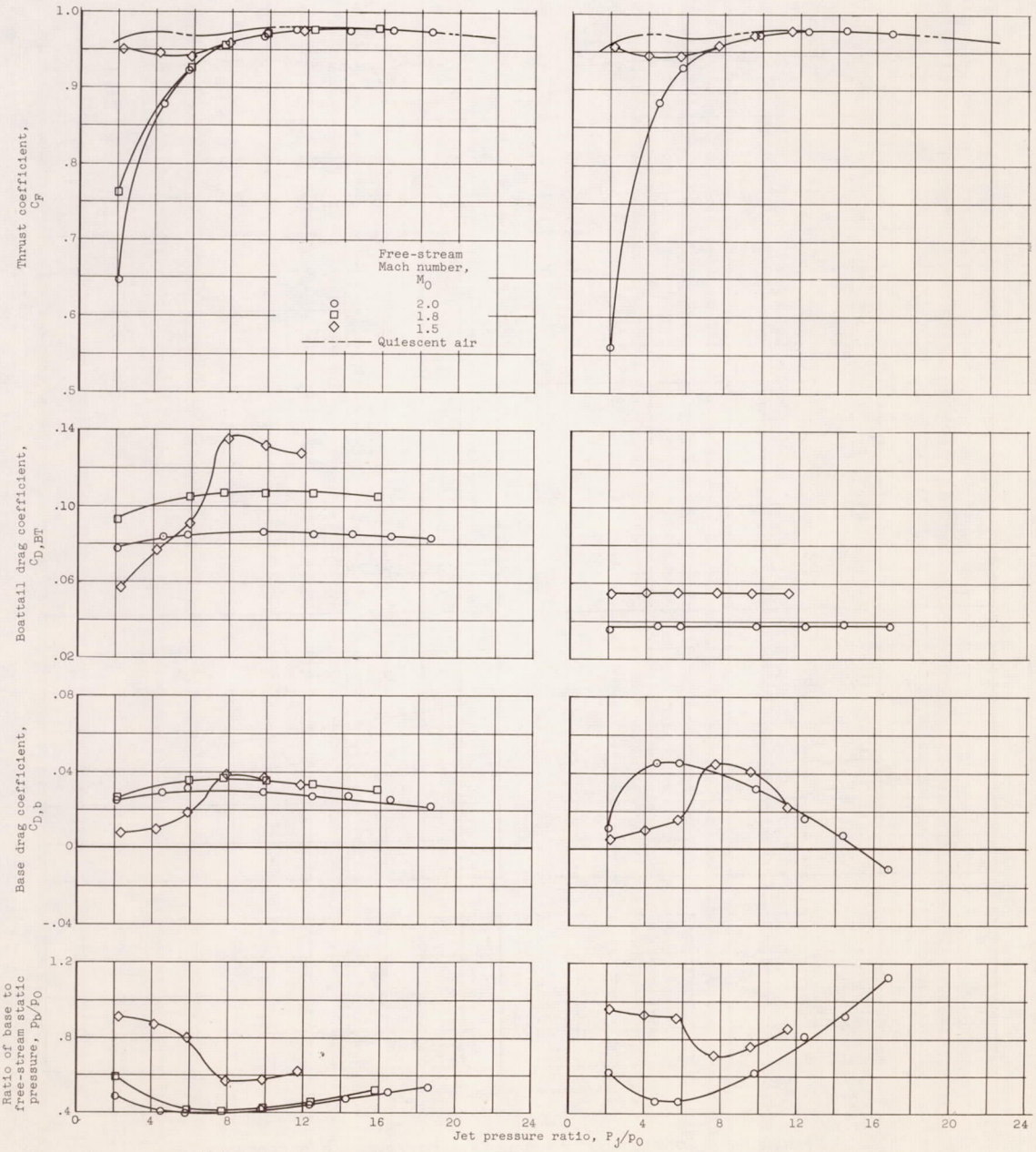

(g) Configuration 15-.2-S.

(h) Configuration 15-.2-L.

Figure 6. - Continued. Plug nozzle performance parameters.

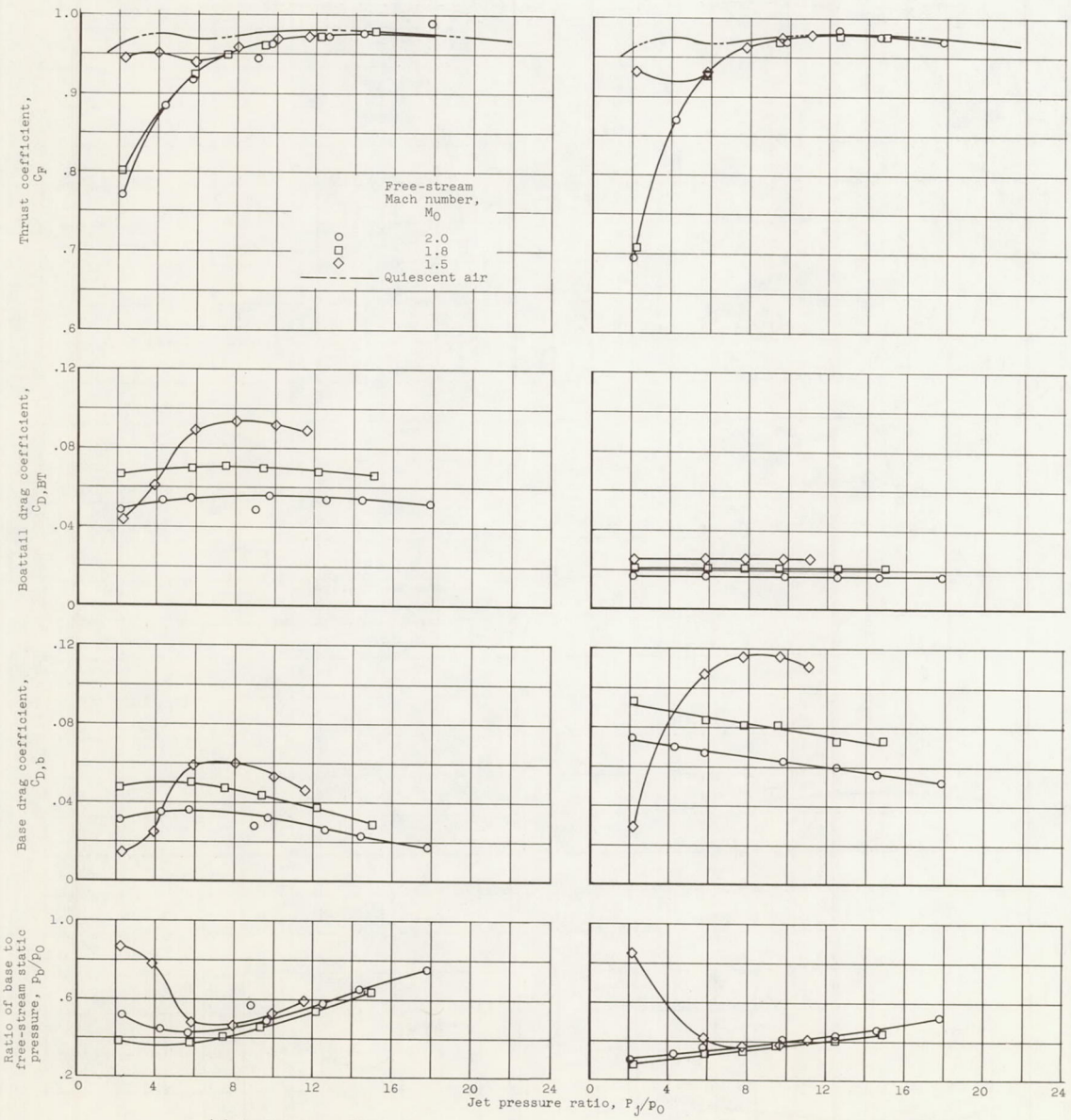

(i) Configuration 15-.25-S.

(j) Configuration 15-.25-L.

Figure 6. - Continued. Plug nozzle performance parameters.

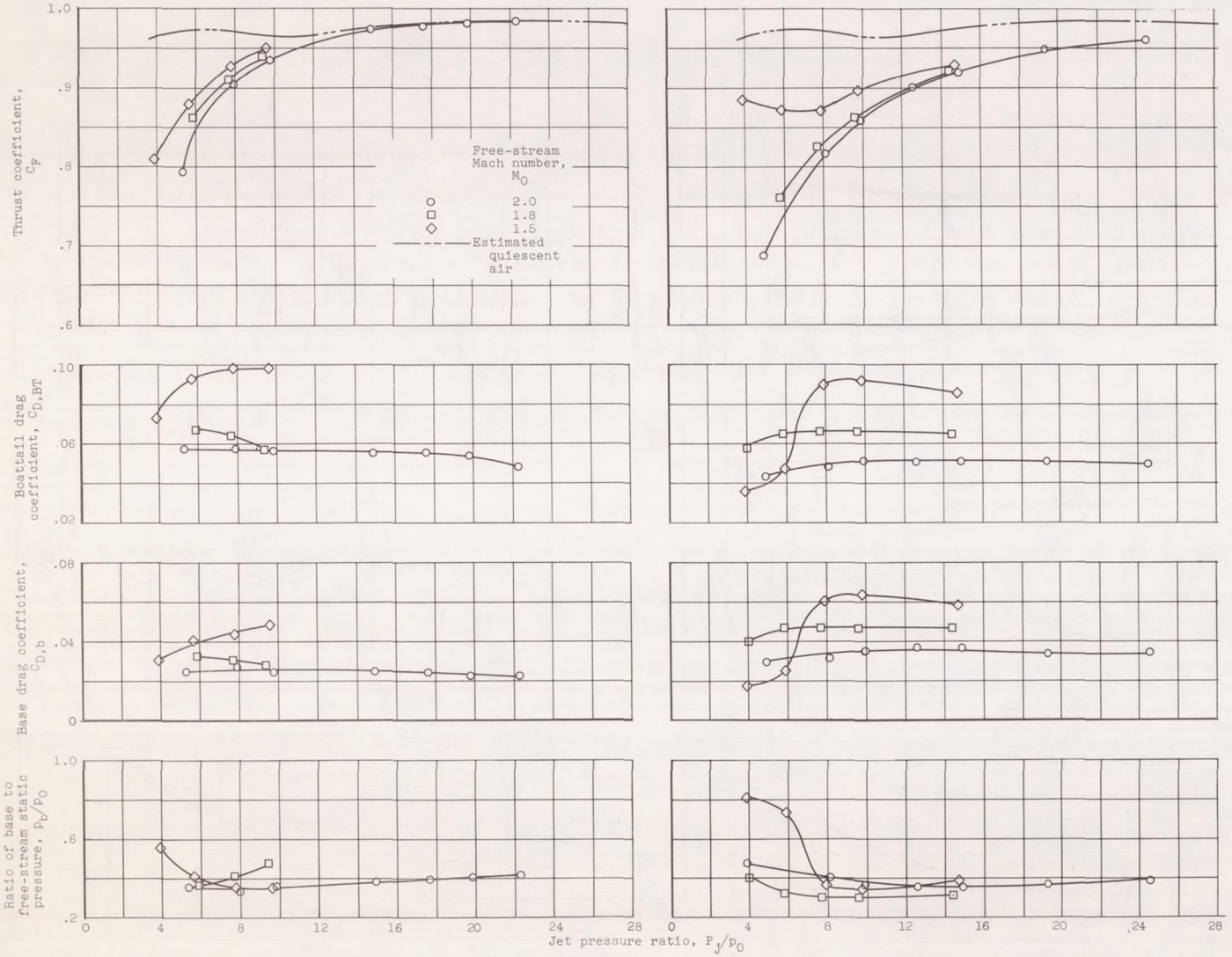

(k) Configuration 25-.2-S.

(l) Configuration 25-.14-SA0.

Figure 6. - Continued. Plug nozzle performance parameters.

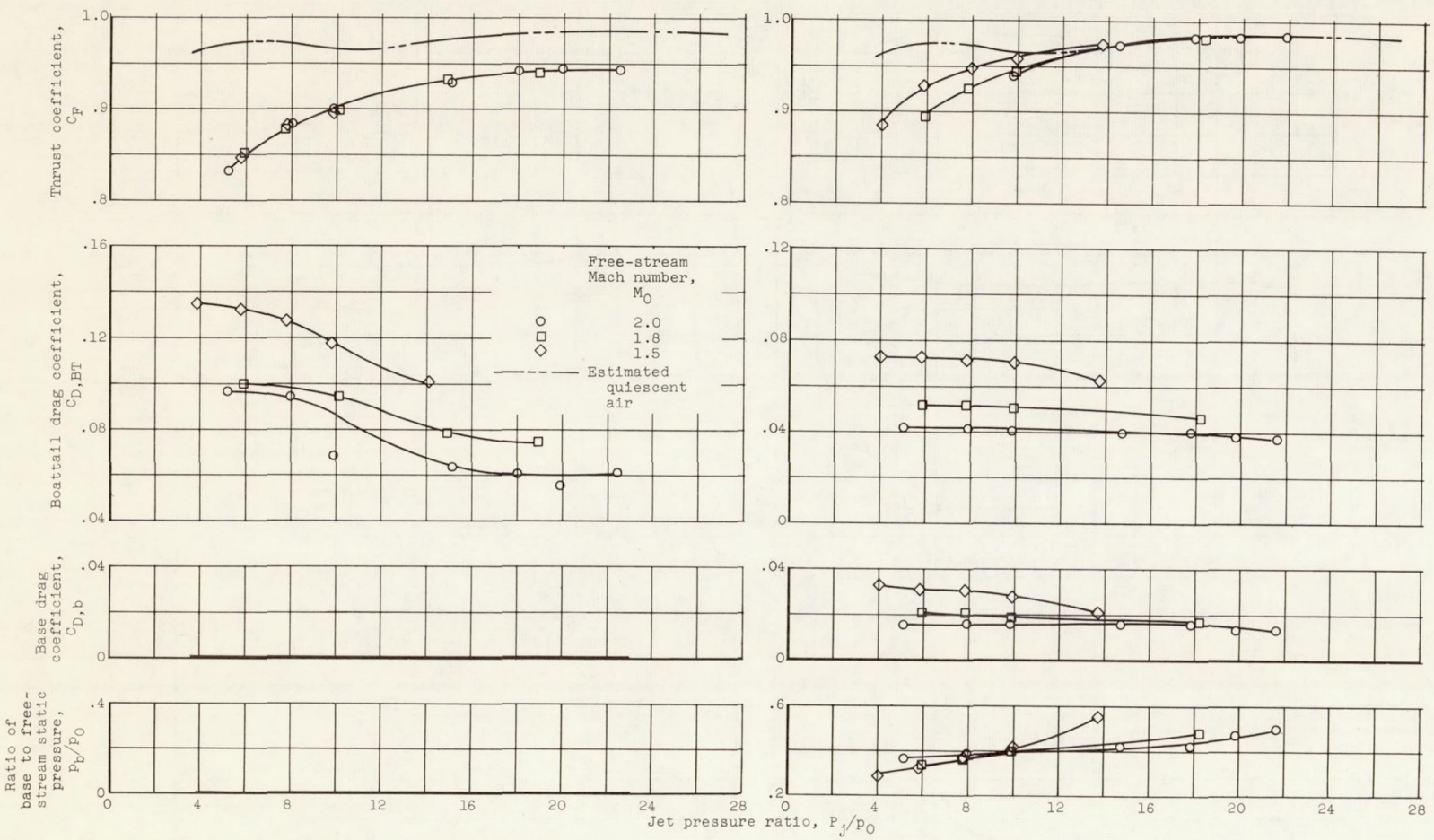

(m) Configuration 25X-.2-0.

(n) Configuration 25EI-.2-S.

Figure 6. - Continued. Plug nozzle performance parameters.

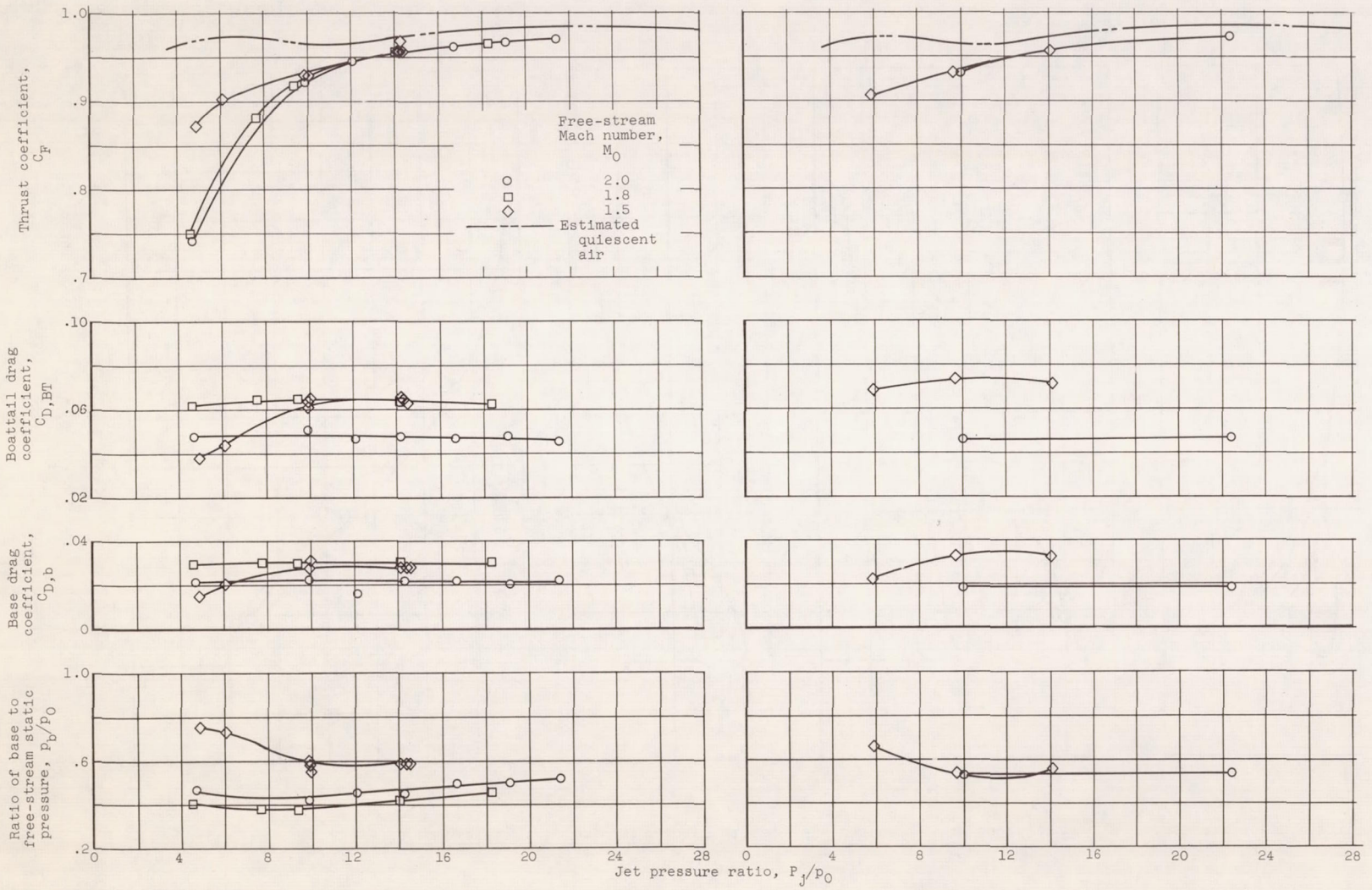

(o) Configuration 25-.2-S (8-in. flat ring).

(p) Configuration 25-.2-S (8.5-in. flat ring).

Figure 6. - Continued, Plug nozzle performance parameters.

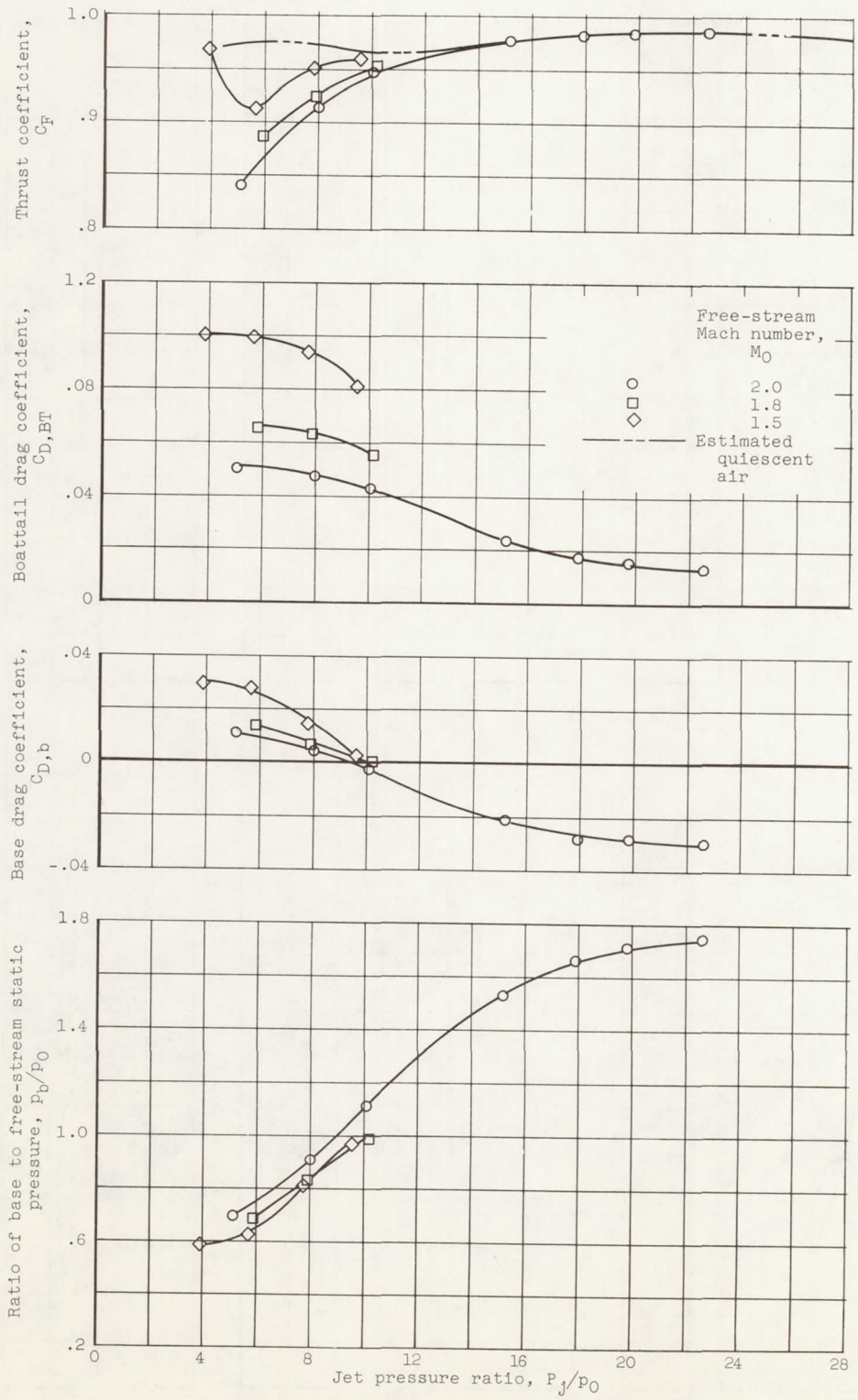

(q) Configuration 25-.2-S (contoured ring).

Figure 6. - Concluded. Plug nozzle performance parameters.

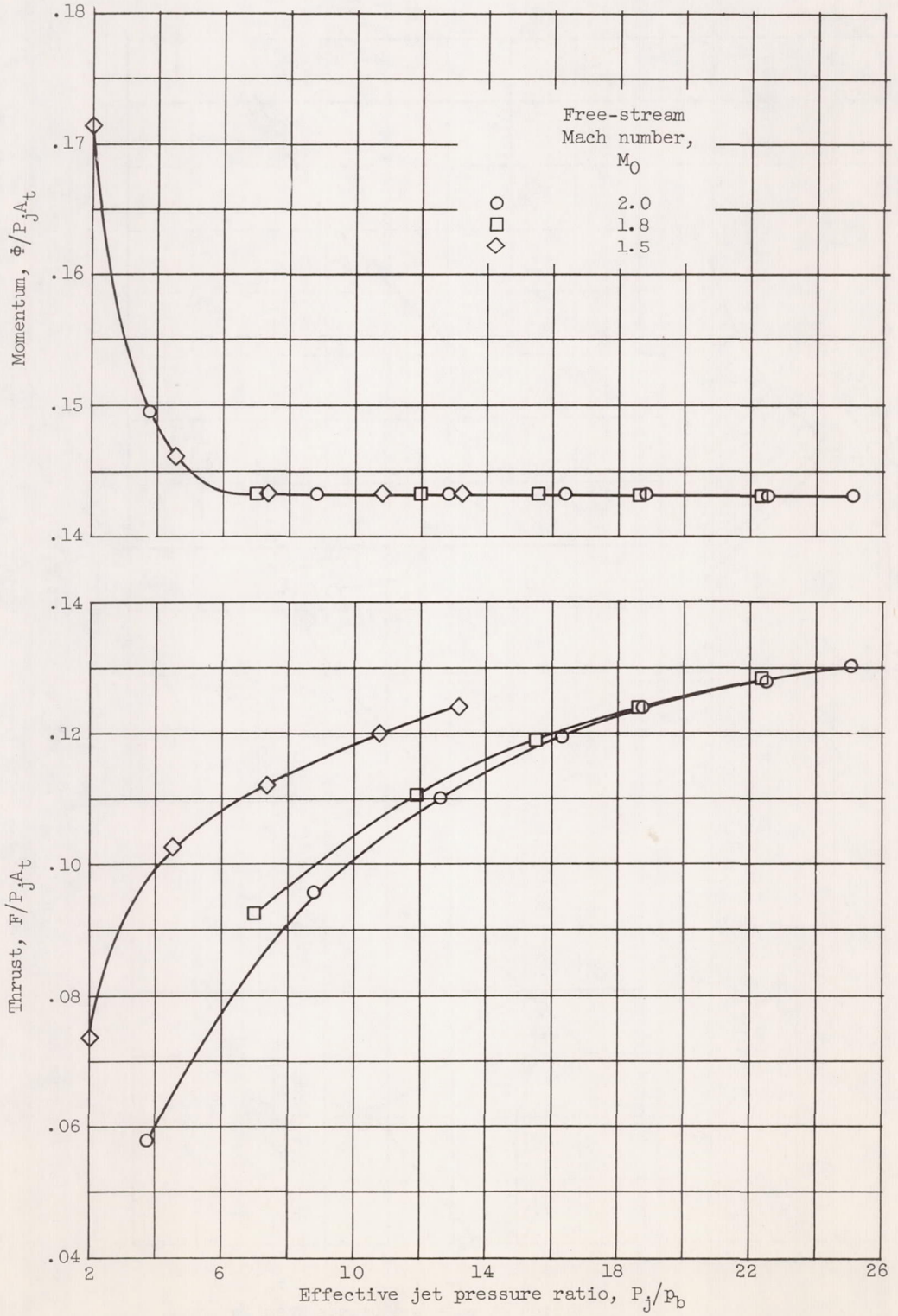

Figure 7. - Correlation of exit momentum by means of "effective pressure ratio." Configuration 10-.2-S.

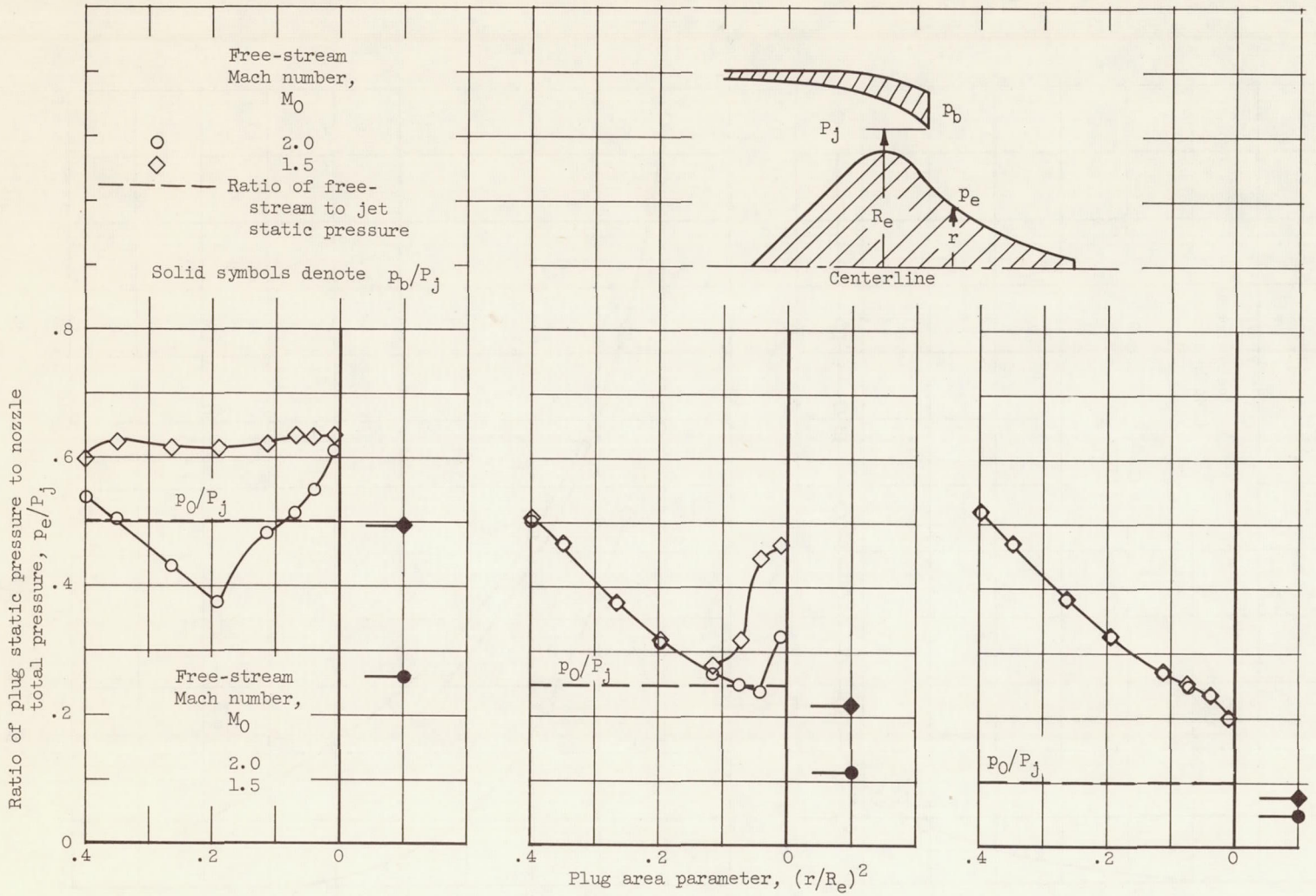

(a) Jet pressure ratio, ~2. (b) Jet pressure ratio, ~4. (c) Jet pressure ratio, ~10.

Figure 8. - Typical plug pressure distributions. Configuration 10-.2-S.

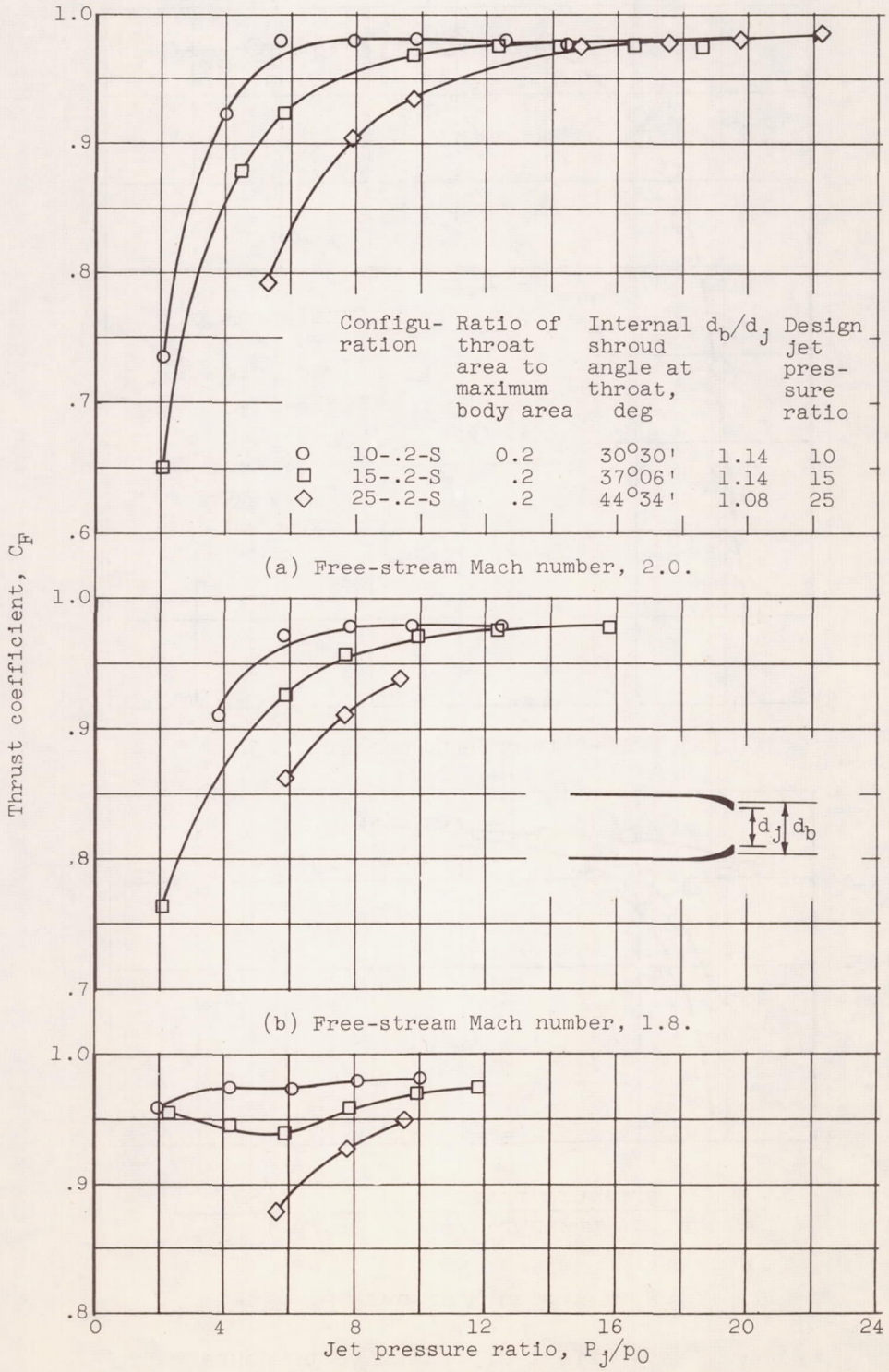

(a) Free-stream Mach number, 2.0.

(b) Free-stream Mach number, 1.8.

(c) Free-stream Mach number, 1.5.

Figure 9. - Effects of design pressure ratio on nozzle performance.

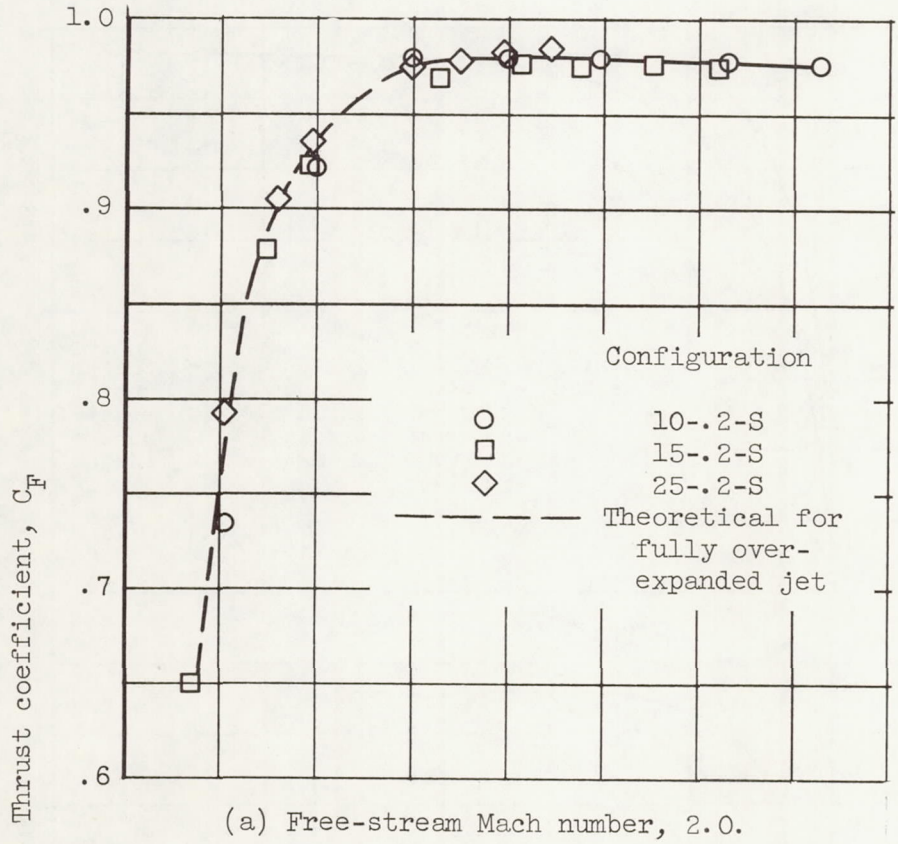

(a) Free-stream Mach number, 2.0.

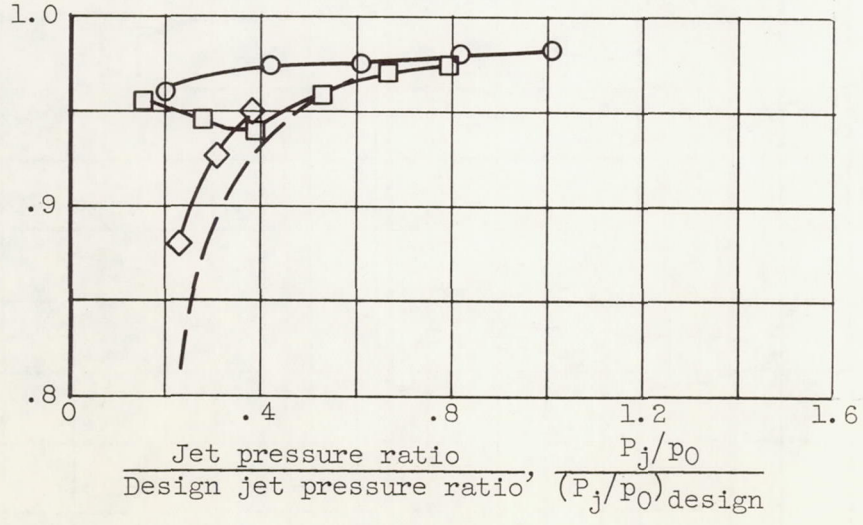

(b) Free-stream Mach number, 1.5.

Figure 10. - Effect of "relative pressure ratio" on thrust.

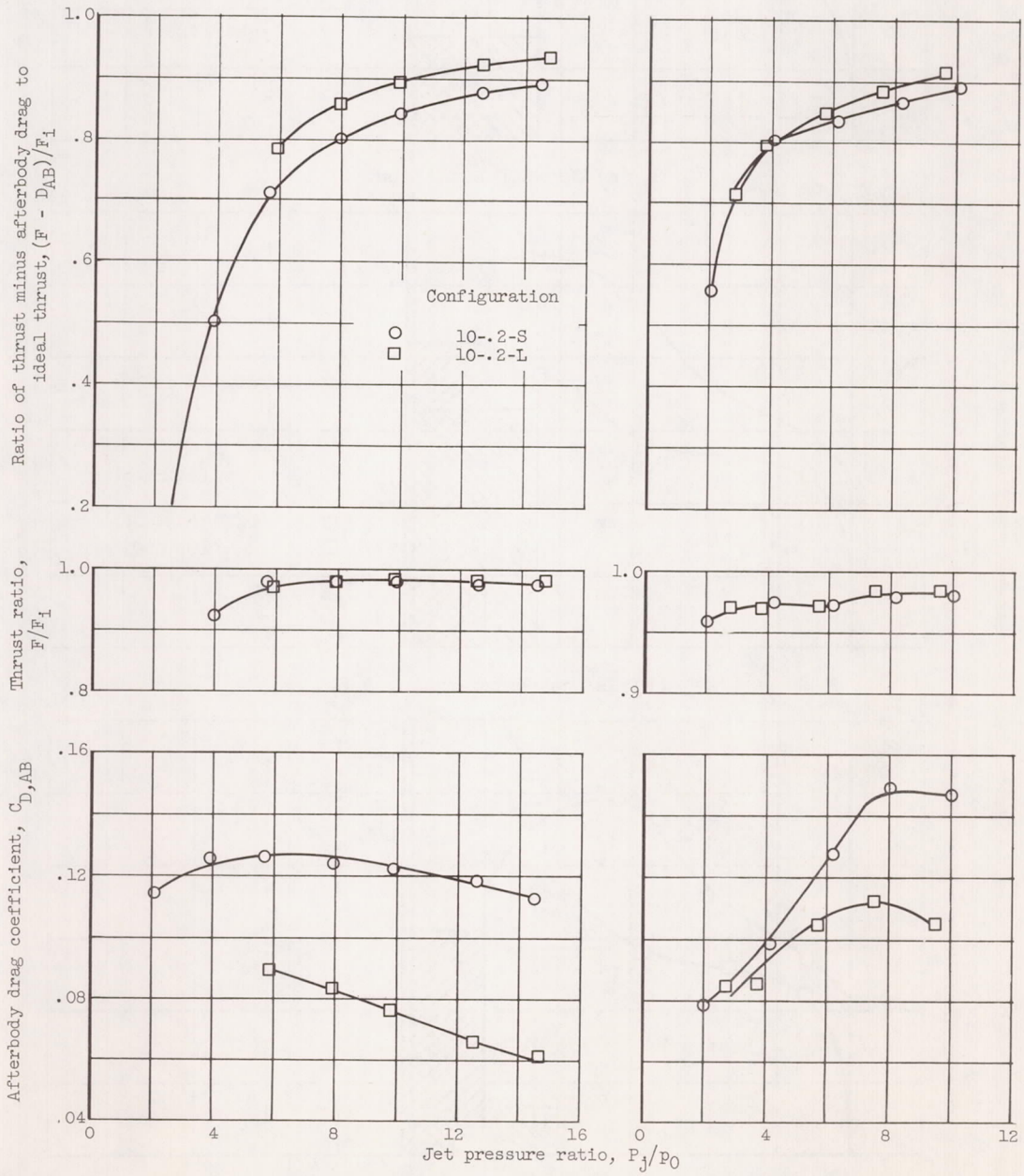

(a) Free-stream Mach number, 2.0.

(b) Free-stream Mach number, 1.5.

Figure 11. - Typical effects of afterbody shape on nozzle performance.

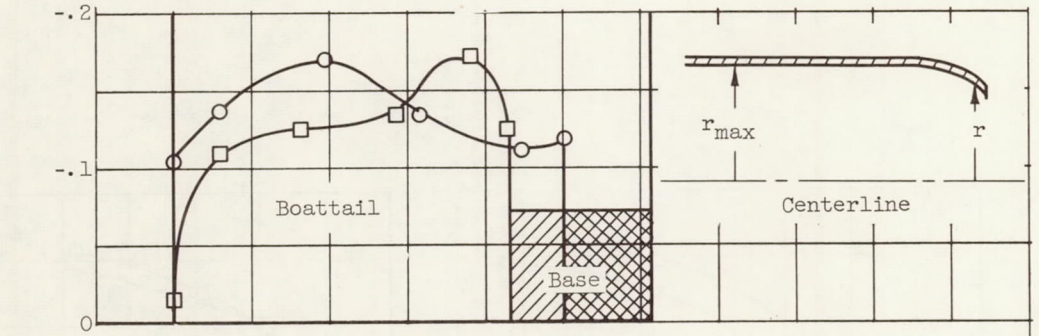

(a) Jet-off condition.

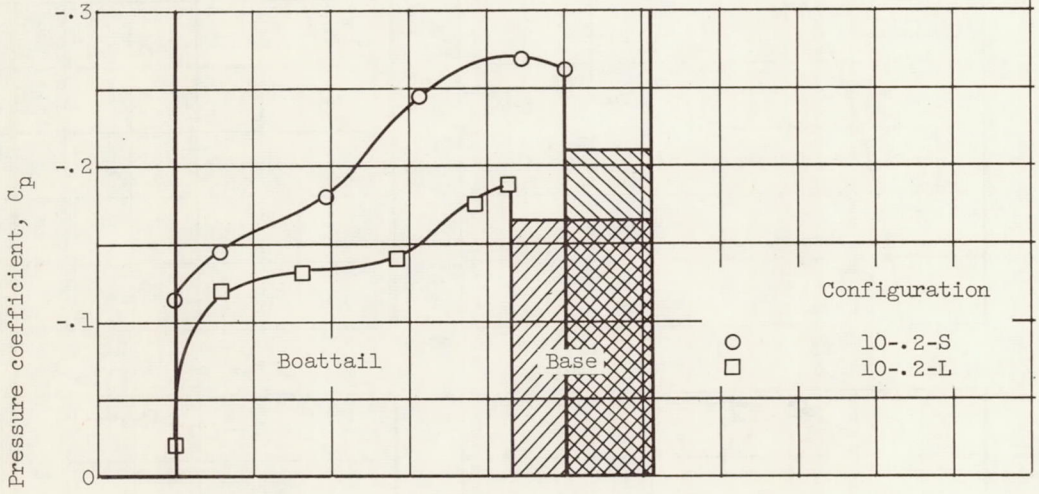

(b) Jet pressure ratio, ≃ 6.

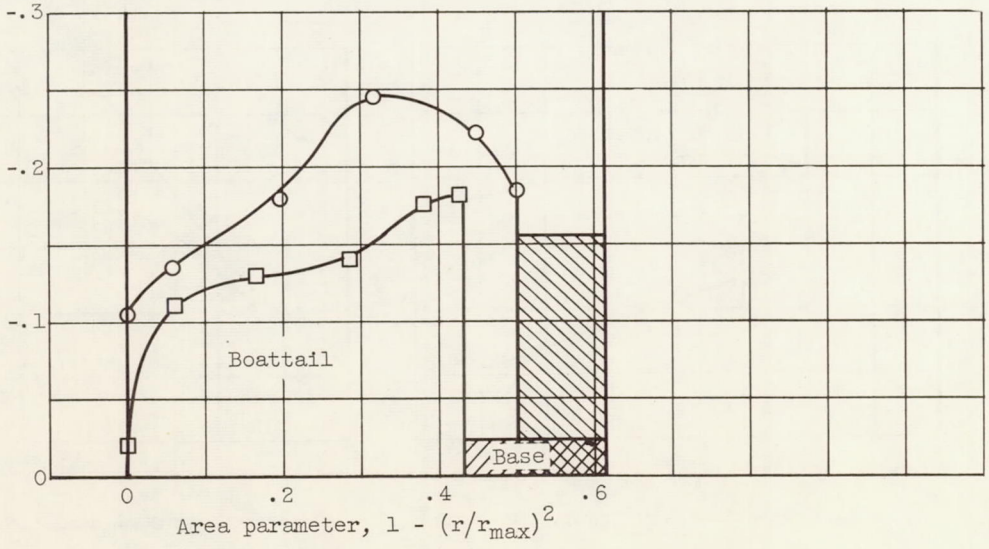

(c) Jet pressure ratio, ≃ 15.

Figure 12. - Boattail pressure coefficients. Free-stream Mach number, 2.0.

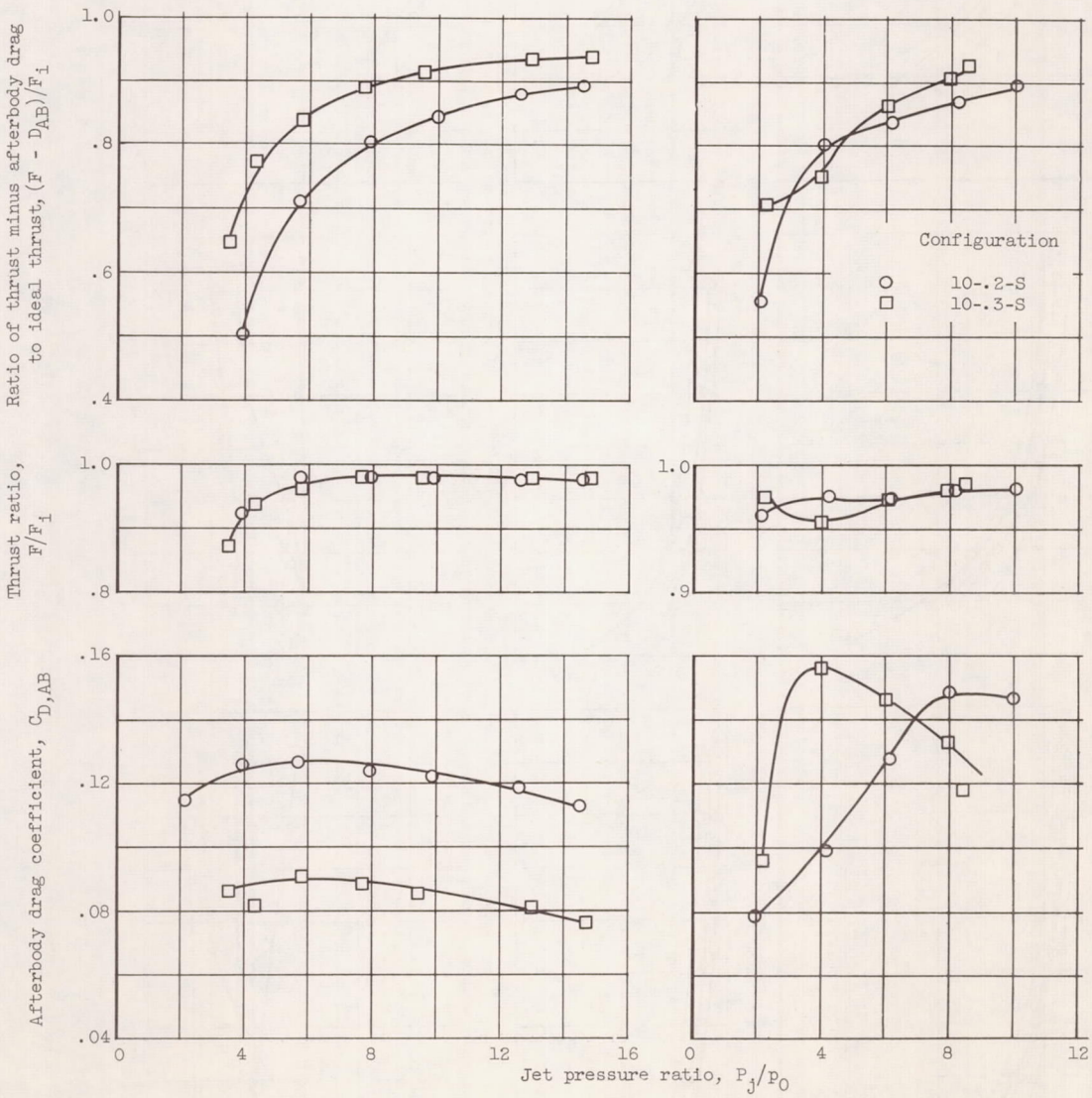

(a) Free-stream Mach number, 2.0.

(b) Free-stream Mach number, 1.5.

Figure 13. - Typical effects of ratio of throat to maximum body area ratio on nozzle performance.

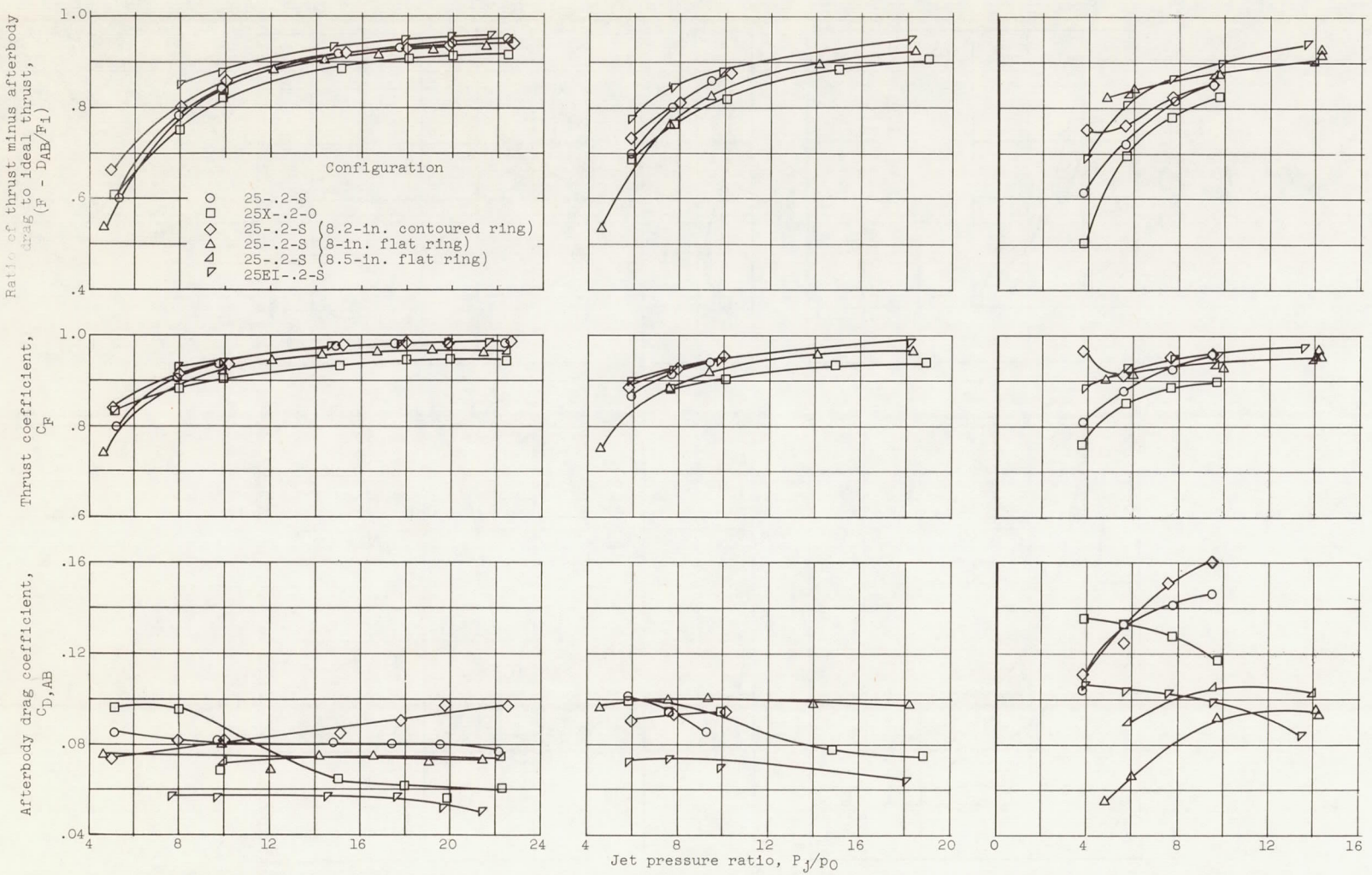

(a) Free-stream Mach number, 2.0. (b) Free-stream Mach number, 1.8. (c) Free-stream Mach number, 1.5.

Figure 14. - Comparison of nozzle performances of configurations designed to operate at jet pressure ratio of 25.

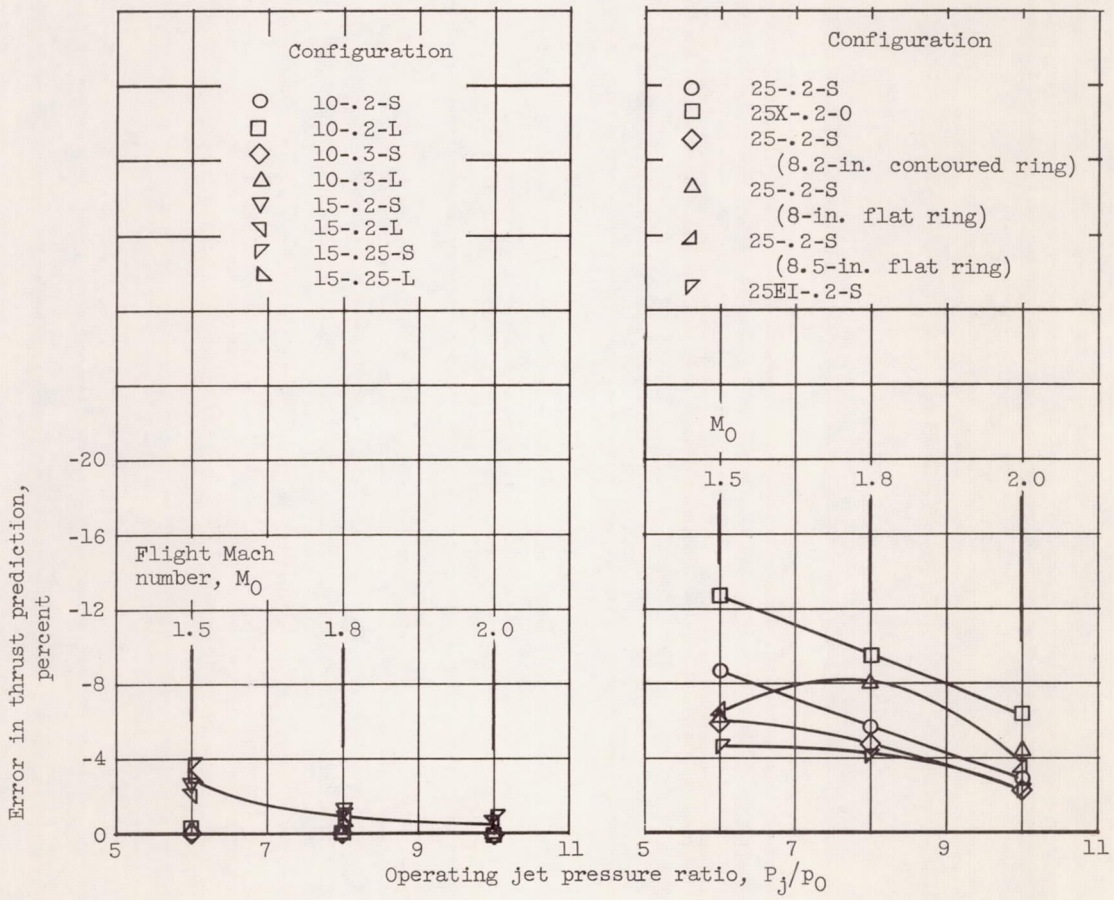

(a) Design jet pressure ratio, 10 and 15.

(b) Design jet pressure ratio, 25.

Figure 15. - Error in predicting configuration gross jet thrust from quiescent-air data.